12-19-2022

Exploring the Binding of Anticancer Drug BI-3802 with DNA Using Optical Tweezers

Jared McAuliffe
Bridgewater State University

Exploring the Binding of Anticancer Drug BI-3802 with DNA Using Optical Tweezers

Jared McAuliffe

Mentor

Dr. Thayaparan Paramanathan

Submitted in Partial Completion of the

Requirements for Departmental Honors in Physics

Bridgewater State University

December 19, 2022

Exploring the Binding of Anticancer Drug BI-3802 with DNA Using Optical Tweezers

Jared McAuliffe

Submitted in Partial Completion of the
Requirements for Departmental Honors in Physics

Bridgewater State University

December 19, 2022

Dr. Thayaparan Paramanathan, Thesis Advisor	Date: 12/23/22
Dr. Edward Deveney, Committee Member	Date: 12/24/22
Dr. Elif Demirbas, Committee Member	Date: 12/23/22

Table of Contents

Acknowledgements

In 2020 when I finally gained the courage to leave my full-time job to return to full-time studies, I truly never imagined myself sitting here, right now, writing an honors thesis. It has been an amazing journey that has led me to this point, and I owe thanks to the kindness and support of many amazing people. My first experience with Bridgewater State University was the summer STEM transfer program led by Dr. Alexandra Adams. I want to thank “Mrs. Dr. Adams” for the perfect introduction into the BSU family, her enthusiasm for the university and passion for student success was my first sign that BSU was different than other universities.

It was Dr. Alexandra Adams who introduced me to my college mentor who was so much more than a mentor, Dr. Thayaparan Paramanathan. Dr. Thaya, as he thankfully allows students to call him, has been a godsend in my life. It is hard to find the words to describe the man Dr. Thaya is, but it is easy to say he always puts his students success first and foremost. This was evident in the weekend meetings we would have when a deadline was looming, or just our normal “one hour” weekly meetings that would stretch on for hours into the night drilling in physics concepts or just talking about life. It is easy to say that I am not just a better student for meeting Thaya but a better person as well, so Thaya truly I thank you.

Dr. Thaya was my first introduction into the BSU physics department, and I assumed he was an outlier, I was blown away when I discovered his peers in the department shared his passion for student success. Two of those faculty members, Dr. Deveney and Dr. Demirbas, are part of my thesis committee so I want to thank them for their time and insight on the edits they have supplied, this thesis is better for it. I always looked forward to taking classes with Dr. Deveney his

enthusiasm for science as a whole coupled with his far-reaching knowledge led the class into countless thought-provoking and stimulating discussions, his courses were always captivating so thank you Dr. D. Thank you to Dr. Demirbas who encouraged my love for optics and broadened my understanding of the subject. I want to thank Dr. Kling, as the physics department chair, he seems to always find a way to get things done going above and beyond for his students inside the classroom and out. Thank you to Dr. Williams who could bring humor into the hardest of physics topics and wears his love of physics on his sleeve, which was contagious. Dr. Hernandez thank you for taking the time to diagnose my first couple circuits in the electronics course as they looked like bird nests. Thank you to the former dean Dr. Porter-Utley who advocated so strongly for the success of her students and my lab which allowed me to attend the 2022 annual Biophysics conference and thank you to the new dean Dr. Ardnt who has so seamlessly filled into her role. Thank you to the administrative assistant Patty Benson for being the backbone of physics department, a friendly face, and a true friend. Also, a general thank you to the physics department as a whole, faculty and students, for being a close-knit family and always pushing each other to succeed.

For supporting and funding my research from travel and semester grants to the incredible Adrian Tinsley Program I want to thank BSU's undergraduate research leadership team: Dr Shanahan, Dr. Ken Adams ("Mr. Dr. Adams"), Dr. ingle, and Ms. Kacey O'Donnell. A special shoutout to Dr. Shanahan, thank you for advocating for me to get the funds needed to travel to the Biophysical society annual meeting, I know it was a fight. For his consistent work in providing the Single Molecule Biophysics lab with Flow-cell spacers, a big thanks to Rob Monteith. I want to thank Dr. Steve Haefner and the Chemistry Department for providing me with the use of their -80° freezer

and use of their Milli Q water. I would be amiss without thanking all the former SMB lab members for paving the way for the research I was able to conduct. Special thanks to former SMB lab member Joshua Watts for showing me the ropes, sharing your immense knowledge, training me in the basic skills for conducting research, and being a good friend. Thank you to all the current lab members for continuously asking questions, keeping me on my toes, and inspiring me to be my best as a lab role model. I want to thank Dr. Williams from Northeastern University as well as Dr. Rouzina from The Ohio State University for their collaboration, feedback, and expert insight on this project.

I would have never succeeded without my lifelong support system. I, of course, want to thank my mother for her unwavering support in all my undertakings, as an untraditional student yourself your advice was always valid and appreciated. Thank you to my older brothers Josh and Jake and younger brother Shane for their support, advice, and belief in me. It's nice to know you all are just one phone call away. I want to thank my girlfriend Alison Conley and my best friend Sam Clark for always hyping me up, coming to my presentations, and picking me up when I was feeling down. Lastly, I want to take a moment to remember my father who passed away from cancer in 2014, you are never far from my thoughts, and I know you would be proud of this project and my accomplishments.

Abstract

BI-3802 is a relatively new anticancer drug known to bind to the transcription repressor BCL6 which can lead to the regression of the most common form of cancer in the lymphatic system, B-cell lymphoma. Based on the structure of BI-3802 we believe this small molecule drug can bind to DNA through intercalation. Intercalators are a special type of molecule which have a flat planar section that can stack between DNA base pairs. In this study, we use Optical tweezers to trap a single DNA molecule in order to explore the binding of BI-3802 with DNA. Once we trap a single DNA molecule, we stretch the DNA and measure the tension in the DNA as a function of extension. During this process, at a certain force, the DNA undergoes a phase transition from double stranded DNA (dsDNA) to single stranded DNA (ssDNA). DNA stretching is repeated in the presence of various concentrations of BI-3802 in order to study the interaction between the drug and DNA at the molecular level. Our results suggest that the force where the phase transition from dsDNA to ssDNA occurs is decreased as the concentration of BI-3802 is increased, indicating this drug destabilizes the naturally occurring double stranded structure of DNA at micromolar concentrations. To our knowledge this is the first study that explores the interactions of BI-3802 with DNA at the single molecule level. The outcome of these experiments may help us better understand drug interactions at the molecular level and help develop new therapeutics.

Introduction

DNA

Every human is made of trillions of building blocks called cells, and in every cell, there is a molecule known as DNA (Deoxyribonucleic acid). DNA is essential for the function of a cell as it contains the instructions for an organism to reproduce and survive. There are numerous companies and businesses of recent years such as "23andMe" that use DNA to link genealogies and track ancestry making DNA a commonplace topic in our modern society. These days the concept of DNA is taught from a young age but in the early 20th century the molecule responsible for carrying our genetic information was a mystery to the scientific world. In 1865 Gregor Mendal, an Austrian monk performed an experiment where he created multiple generations of pea plants in order to better understand the workings behind inheritance. Using pea plants with different traits such as flower color he could control pollination and track the rate of inherited traits through several pea plant generations. His findings led to his creating of the particle theory of inheritance[1]. The particle theory of inheritance states that there are genetic units that determine the traits passed on through generations, today we know these genetic units to be genes[2].

More than 60 years later in 1928, while studying a pneumonia causing bacteria, British bacteriologist Fred Griffith performed an experiment that pointed to DNA as the carrier of genetic information although at the time there was still much doubt on Griffiths findings[3]. This was until 1944 when the team of Oswald Avery, Colin MacLeod, and MacLynn McCarty built on the work of Griffith further demonstrating that DNA was in fact responsible for inheritance[3,4].

In April of 1953 there was a major breakthrough[5-7]. Four scientists, Maurice Wilkins, Rosalind Franklin, James Watson, and Francis Crick (*Figure 1*) are credited with the discovery of the three-dimensional DNA structure we know today. This discovery was largely due to the work of many scientists before them such as Friedrich Miescher, Phoebus Levene, and Erwin Chargaff. Thanks to these great minds we have a clear picture of the structure of DNA[8].

Figure 1: Images of the scientist mainly credited for discovering the three-dimensional molecular structure of DNA (Deoxyribonucleic acid) from left to right James Watson, Francis Crick, Maurice Wilkins, and Rosalind Franklin. Photo credit: Cold Spring Harbor Laboratory Library and Archive, James D. Watson Collection.

The DNA structure consists of two long strands made of sugar-phosphate, known as the DNA backbones, coiled around each other to create a twisted ladder shape (*Figure 2*)[8], known as a double helix[5,6]. Each strand is built from four different nucleotides: Adenine (A), Guanine (G), Thymine (T), and Cytosine (C)[9], which are what carry our genetic information. The two strands, separated by 2 nanometers (nm), are connected by pairings between the nucleotide bases; this can be imagined as rungs connecting the two rails of a twisted rope ladder. These base pairings are specific; adenine only pairs with thymine and guanine only pairs with cytosine[10]. Nitrogenous base pairs (the rungs of the ladder) are separated by a distance of 0.34 nm[1]. The twisting nature

of the double helix creates repeating major and minor grooves in the structure. One full turn of DNA helix (known as a pitch) has approximately 10 base pairs and is 3.4 nm in length.

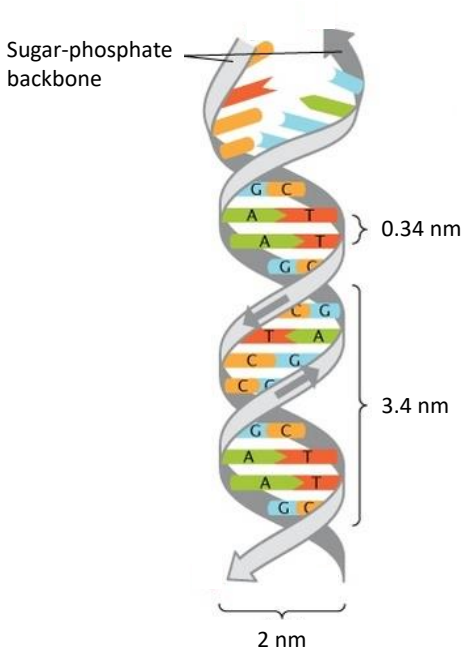

Figure 2: Cartoon representing the double helix structure of DNA, with color-coded nucleotides (A, T, G, C) and gray sugar-phosphate backbones. The double helix contains major and minor grooves. (Adapted from reference 9)

The central dogma of biology is governed by three main processes: DNA replication, DNA transcription into RNA (A similar molecule to DNA but with a single strand, we will discuss in detail later), and the translation of RNA into proteins. For our project we are only interested in the processes of replication and transcription since our drug BI-3802 is known to interact during these processes[11].

Replication

Cells in our body are constantly being replaced with new cells by dividing one cell into two daughter cells[1]. Each new cell needs DNA to function, the process of making two copies of DNA is known as replication (Figure 3). The first step in replication is for helicase, a motor protein, to open the double helix and separate the two DNA strands, this is done to read and copy the nucleotide bases. Then an enzyme known as DNA polymerase binds to each strand to read and add complementary bases to both strands, resulting in two new DNA molecules.

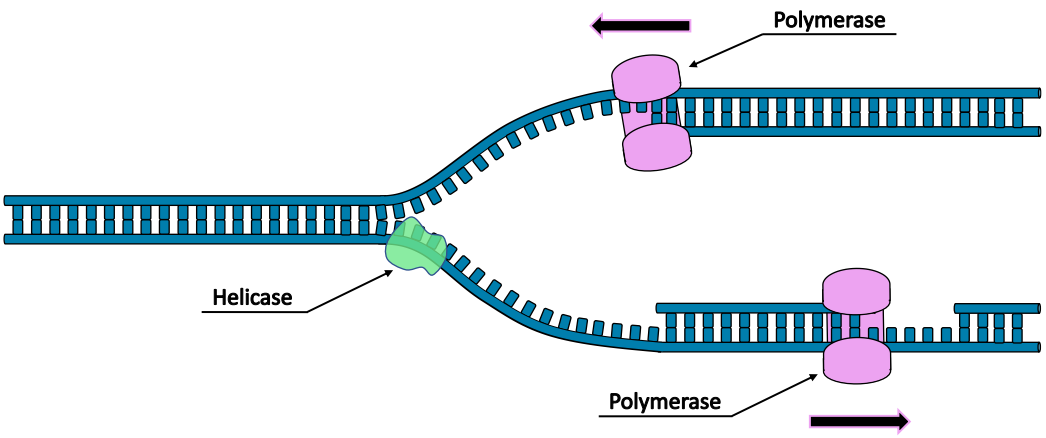

Figure 3: Cartoon illustrating the process of replication where one DNA double helix (left) is being opened by helicase (green) and read by DNA polymerase (pink) to create two new DNA molecules (right).

Transcription

Transcription is the process in which segments of a DNA molecule are transcribed into RNA molecules[1]. RNA nucleotides differ slightly from that of DNAs. The four RNA nucleotides are Adenine, Guanine, Cytosine, and Uracil which replaces Thymine. A particular type of RNA known

as messenger RNA (mRNA) controls protein synthesis and regulation[1]. Transcription occurs in three distinct steps: initiation, elongation, and termination. During initiation, an enzyme known as RNA polymerase binds to what is known as the promoter region of DNA (Figure 4).

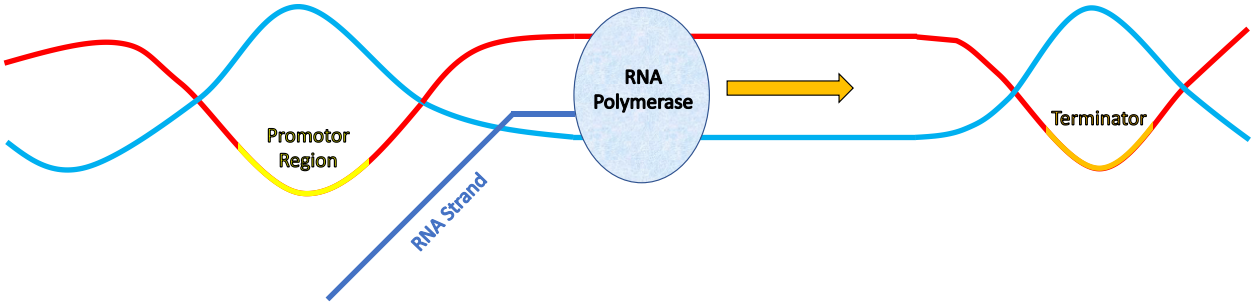

Figure 4: Cartoon illustrating the process of transcription. The RNA polymerase (light gray oval) is seen after it has bound to the promotor region (yellow) the DNA segment where the transcription begins (initiation). The RNA polymerase is seen here during the elongation step unzipping the DNAs two strands (red and light blue) creating the bubble and synthesizing an RNA strand (blue) along the way. The polymerase is moving towards another DNA sequence called the terminator (orange). The terminator will signal to the polymerase that it is time to be released (termination step) effectively ending the transcription process.

The promoter region is a small DNA sequence that can be recognized by proteins called transcription factors, which help the RNA polymerase to bind. Once the RNA polymerase binds to the promoter region it unzips the double stranded DNA forming what's referred to as a bubble. It then reads the template strand and synthesizes an mRNA as it goes along the elongation step. The elongation step is ended when the RNA polymerase reaches a DNA segment known as the terminator. The terminator signals to the RNA polymerase that it is time to be released, effectively ending the transcription process.

50 - 70 billion cells die in our body die every day and each cell must be replaced[12]. During the process of creating these new cells, replication and transcription occur billions of times and may

not always be perfect. Even after many error checking mechanisms, an error in these processes can lead to many different complications and prevalent among those is cancer.

Cancer: A Silent Killer

Cancer, a word associated with dread, a widespread disease that has impacted us all in some way or another. According to the National Cancer Institute, cancer is a disease in which some of the body's cells grow uncontrollably and spread to other parts of the body. As stated earlier the body is made up of trillions of cells and due to the numerous types of cells, cancer can start almost anywhere in the body but most commonly effects the skin, bones, blood, brain, breasts, and lungs. Abnormalities in cell division are often caught and stopped by our immune system but sometimes damaged cells can be allowed to multiply unchecked, leading to a lump of tissue known as a tumor. Tumors can be cancerous (malignant) or non-cancerous (benign). Cancerous tumors have the ability to invade nearby tissues and can use the bodies pathways to spread and form new tumors in a process called metastasis.

Lymphatic Cancer and Transcription Repressor BCL6

Lymphoma is a cancer of the lymphatic system (Figure 5)[13], which is part of the body's germ-fighting network. The lymphatic system includes the lymph nodes (lymph glands), spleen, thymus gland, and bone marrow. Lymphoma can affect all these areas as well as other organs throughout the body. B-cell lymphoma is the most common type of lymphoma that originates from B-cells,

a type of white blood cell that makes antibodies. About 85% of all lymphomas in the United States are B-cell lymphoma[14].

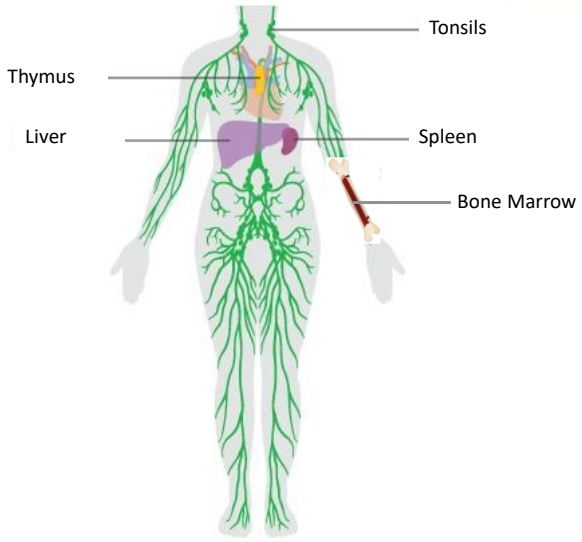

Figure 5: Cartoon image of a human body displaying the parts of the lymphatic system highlighting the tonsils in the neck, the thymus in the chest, the liver and spleen in the stomach, and an example of bone marrow in the arm.

For B-cell lymphoma to materialize it must sneak past the body's defenses, one such defense is the cell checkpoints during the cell cycle. These checkpoints ether allow healthy cells to continue in the cycle or terminate mutated cells such as cancer cells. Certain proteins known as transcription repressors can negatively affect the efficiency of these checkpoints allowing mutated cancer cells to replicate.

Transcription repressors are proteins that bind to specific areas on the DNA and prevent the transcription of DNA into mRNA. One such transcription repressor is B-cell lymphoma 6 protein (BCL6). BCL6 was initially discovered as a cause of cancer in B-cell lymphomas[15].

As discussed in the previous section, B-cells are a type of white blood cell that are part of the immune system. They are proliferated and differentiated into long-lived plasma cells that make antibodies to fight infections[16]. The transcription repressor BCL6 drives the malignant (infectious) phenotype by repressing proliferation of good B-cells and blocking B-cell terminal differentiation. This leads to B-cell lymphoma. One way of combating B-cell lymphoma is through blocking the BCL6 repressor by binding anti-cancer drugs and making them dysfunctional, one such drug developed in 2016 is BI-3802.

BI-3802: Targeting BCL6

Most anticancer drugs fall into the category of small molecules, which weigh less than 900 Daltons[17] (Dalton is a unit used to measure mass in chemistry, one Dalton is approximately 1.66×10^{-27} kg). BI-3802 is a recently developed small molecule drug that binds to the transcription repressor BCL6 (described above) in a highly specific and reversible manner[11]. If BCL6 is overexpressed in certain blood cells it can lead to the development of B-cell lymphoma. Turning off BCL6 in these cells could lead to the regression of the disease and that is the intent of the drug BI-3802[11]. Based on the molecular structure

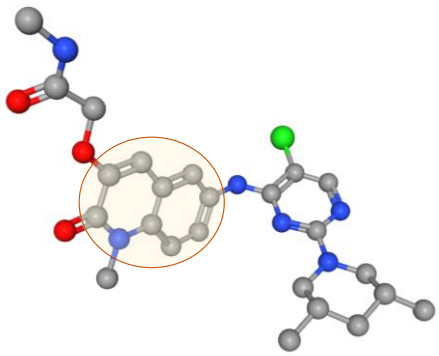

Figure 6: Ball and stick model representing the structure of anticancer drug BI-3802, where the planar section expected to intercalate is highlighted in the light-yellow circle.
(Adapted from NCBI Database SID 346535574)

(Figure 6) this drug looks like an intercalator, a special type of molecule which has a planar section that can stack between DNA base pairs.

Intercalating properties of this drug have not yet been explored to our knowledge. Many intercalators have been studied using optical tweezers to provide molecular-level details of their interaction. Intercalating drugs also have the capability of interfering with the replication process of DNA. The purpose of this research is to use optical tweezers to explore the interactions of BI-3802 with DNA and see whether the it will interfere with replication in addition to transcription.

Optical Tweezers: Trapping with Light

Known in the scientific community as the father of optical trapping, Nobel laureate Arthur Ashkin developed the theory behind this technique during the dawn of laser technology in 1970 over five decades ago[18].

Ashkin's influence was far reaching, in the 1980s, Stevin Chu a scientist who was working in Bell Labs was influenced by Ashkin and led a team in using a laser to cool and trap atoms. This was considered the first optical trap, and for this achievement Chu was awarded the 1997 Nobel prize in Physics[19]. In 1987 soon after the first optical trap was displayed Ashkin and his team solved an important issue, they figured out how to trap biological materials without sample damage. They used a laser with an infrared

Figure 7: Photograph of Arthur Ashkin levitating small particles with a laser beam at Nokia Bell Labs (1971)

wavelength to trap and manipulate viruses and bacteria as this wavelength was less likely to be absorbed by water to produce heat[20].

In the 1990s, driven by Askins discoveries, there were several research groups using optical tweezers to trap numerous types of biological materials including: DNA[21], RNA[22], retinal neurons[23], cartilage cells[24], chromosomes[25], cell membrane[26], red blood cells[27], etc.[22]. Polystyrene beads were trapped in order to catch and manipulate single biomolecules, much like the Bridgewater State University Single Molecule Biophysics lab (BSU SMB Lab) does today[28-31].

Based on his continuous contribution to the field and specifically the breakthroughs optical tweezers have had in biological research Arthur Ashkin was awarded the 2018 Nobel Prize in Physics (he is the oldest person to win the Nobel prize at the age of 96). Since Ashkin was not able to attend the Nobel Prize ceremony, single molecule biophysicists in the USA organized an event for him to deliver his Nobel laureate speech in Aspen, CO. At this event while introducing Ashkin Stanford professor Steven Block said of optical tweezers "It's the closest thing to a tractor beam humans have ever produced".

Physics of Trapping: The Micro Tractor Beam

As Ashkin theorized and later displayed optical tweezers are a device that use a series of optical components to focus light to a micron sized point. This finely focused light can be used to trap and manipulate extremely small particles. Yet some might be wondering like I once was how can light trap anything at all? The actual explanation involves radiation pressure of the light as explained by Ashkin's first paper[32]. In the diffraction limit this can be simply explained with ray

diagrams. In the case of our lab, we are trapping polystyrene beads which are an order of magnitude larger than the lasers wavelength, therefore the trapping can be explained using ray optics.

The first key to explain the trapping is to understand the phenomenon known as refraction and Snell's law that governs refraction. When a beam of light passes from one medium into another (for example from air into water) the light is bent due to the speed of light changes in different mediums. This bending is known as refraction. The degree of bending depends on the change in the speed of light and is related to a constant associated with the medium known as a refraction index. Snell's law provides a formula that relates the angles that beam makes with the normal (perpendicular line to the interface at the point of incidence) in both mediums with their refractive indices.

$$n_1 sin\theta_1 = n_2 sin\theta_2$$

Where n_1 and n_2 are the refraction indexes of the two mediums respectfully, θ_1 is the angle of incident in medium-1, and θ_2 is the angle of refraction in medium-2.

In our experiments, the beads are denser than the surrounding medium meaning they have a higher refraction index, and the beam of light is refracted towards the normal. In the simple case, when the bead is centered about the optical axis of the objective, we have symmetry (Figure 8).

As the purple beam approaches from the surrounding buffer (water like material) it reaches the bead and the beam is then refracted toward the normal because the bead's refractive index is greater than that of the buffer. Upon exiting the bead, the beam re-enters buffer that has lesser refractive index, therefore the beam is refracted away from the normal as per Snell's law. You can see the orange beam has a mirrored effect on the other side of the bead. So, we can now see how the lights path is changed due to Snell's law but how is this light trapping?

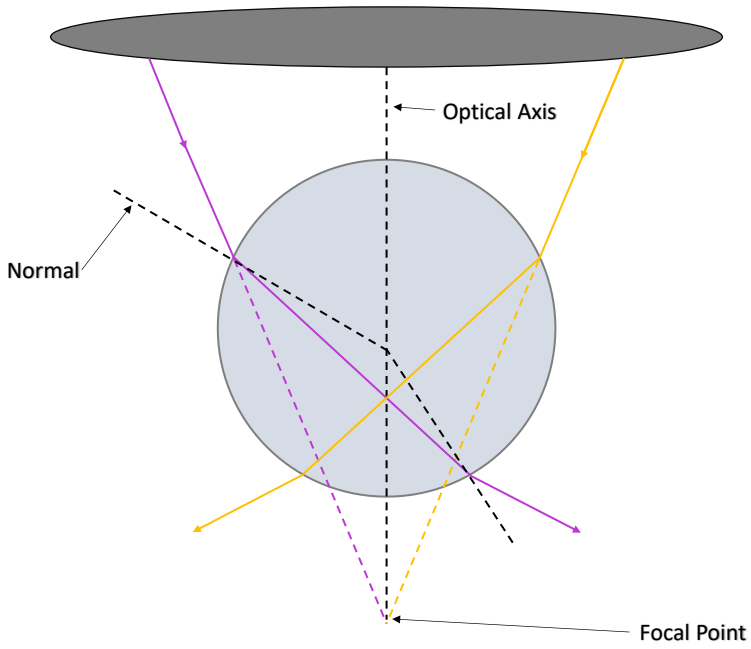

Figure 8: Ray diagram showing the physics behind a bead caught by a laser trap while symmetrically in the optical axis. The laser is focused by the objective (dark gray oval) and is represented by two mirrored rays (solid orange and purple lines). These rays enter the polystyrene bead (light gray circle) which has a higher refraction index causing the lasers to refract and bend towards the normal (black broken line). They are once again refracted while leaving the bead now away from the normal. Doted orange and purple lines show the path the beams would have taken if unaffected by the bead, meeting at the focal point.

Light is made up of tiny particles called photons, due to the light being refracted upon entering the bead these photons experience a change in momentum. The light again is refracted upon exciting the bead creating another change in momentum of the photons. We can use vector addition to predict the direction of the net momentum change and force experienced by these photons (Figure 9).

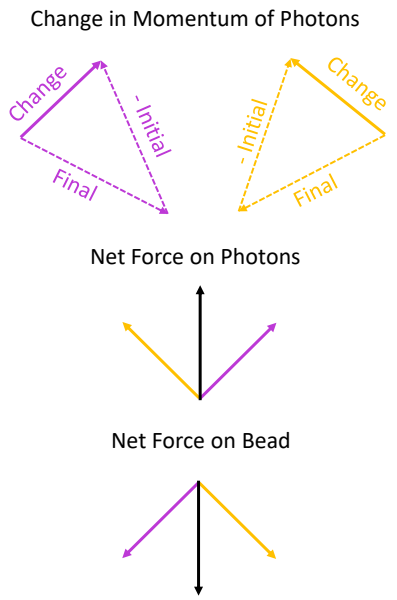

Figure 9: Vector addition showing the change in momentum of photons travelling along the orange and purple beams depicted in figure 8 (top). The forces felt by the photons in each beam are summed to find the net force on the photons (middle). The equal and opposite force felt by the bead (bottom).

As seen in the vector diagram the photons feel a net force in the direction of the objective. Due to newtons third law the bead feels an equal but opposite force due to the photons. In this example the force being applied to the bead is known as the scattering force which pushes the bead in the direction of the laser's focal point.

One of the lasers defining qualities is its gaussian profile, simply this means the intensity of the light is strongest in the middle and the lights intensity gradates to lower intensity on the sides of the beam. When the bead is not along the optical axis of the objective (Figure 10), the beam from the center (maroon) contributes more to the force compared to the beam from the side (pink) and as result the net force now will have a horizontal component in addition to the vertical component. The horizontal component that is caused by the intensity gradient of the laser is known as the "gradient force". You can now see that the gradient force on the bead will push the bead towards the middle of the laser and the scattering force will push toward the focal point.

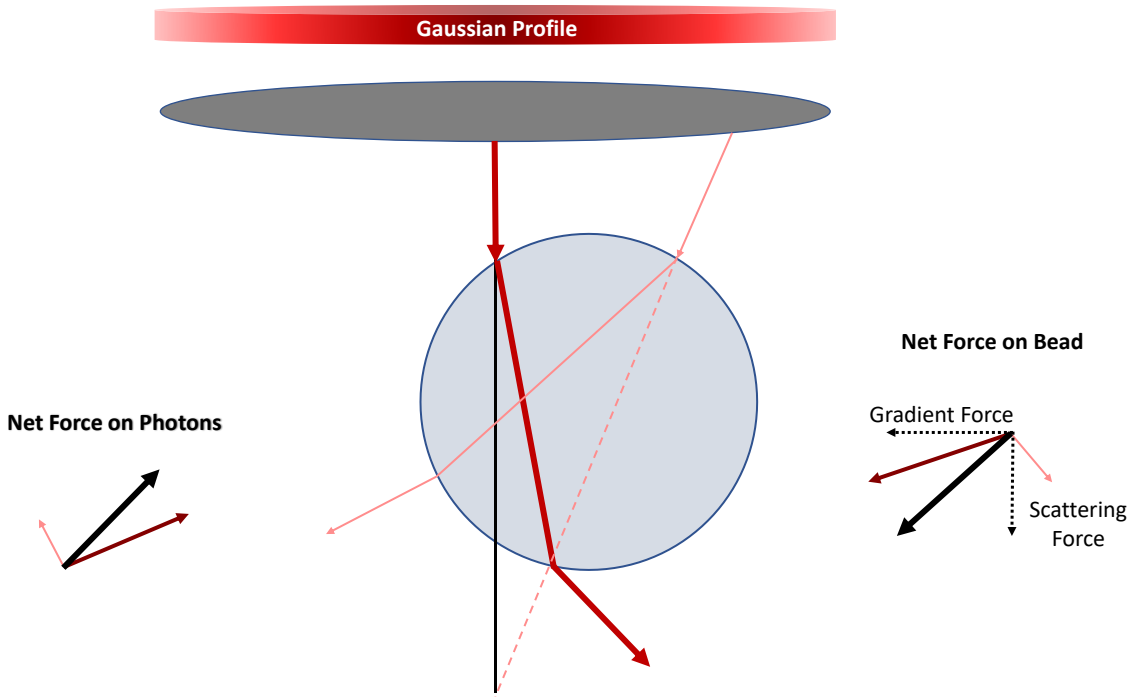

Figure 10: Ray diagram showing a bead caught by a laser trap while off the optical axis. The laser is represented by a gradient-colored cylinder which shows its gaussian profile. After being focused by the objective (dark gray oval) the laser is represented by two vectors: a more intense beam coming from the lasers center (thick, dark red) and a less intense beam coming from the edge of the laser (thin, light red). The beams are refracted through the polystyrene bead (light gray circle). Due to the higher intensity the photons that constitute the dark red beam have a higher momentum change causing more impact on the net force on the photons (left). The net force on the bead will be equal and opposite (right). This results in two components, one that pushes the bead towards the optical axis (gradient force) and the other that pushes it towards the focal point (scattering force).

In the single beam optical trap displayed in the previous figures there would need to be a rigid wall placed opposite the beam in order to prevent the scattering forces from pushing the bead away, or the strength of the gradient force would need to be high enough to tweeze the bead and keep it trapped. In dual beam optical tweezers, there is another equally powered laser beam positioned opposite to the first (counter-propagating), such that the scattering force of each beam cancels out, and the gradient forces add to work as an optical trap. In the Single Molecule Biophysics lab, at BSU we use the dual beam setup to trap polystyrene beads which in order to isolate and manipulate a single DNA molecule and study the interactions of anti-cancer drugs with DNA. These types of studies are known as single molecule techniques.

Isolating and Stretching a Single DNA Molecule

The isolation of a single DNA molecule to stretch and measure the tension in the molecule was first done in 1992 by Steven Smith, Laura Finzi, and Carlos Bustamante with the use of magnetic tweezers. Inside a glass slide they chemically attached one end of a DNA to the slide and the other end to a magnetic bead. They were able to use known magnetic forces to manipulate the magnetic bead and stretch the DNA molecule with up to around 30 pico-Newtons (pN) of force.

Figure 11: Right to left, my mentor Dr. Thayaparan Paramanathan, fellow BSU SMB lab member Joshua Watts, Dr. Laura Finzi the first person to ever stretch DNA, and myself at the 66th Biophysical Society Annual Meeting. (Unfortunately, everyone is wearing masks due to the COVID-19 pandemic)

Then in 1997 a research team led by Steven Block where the first to use optical tweezers to trap and manipulate a single DNA molecule. With this set up they were able to reach around 50 pN of force[21]. Then, in 2001 a team at the University of Minnesota led by Victor Bloomfield used the first dual beam optical tweezers set up to access a much higher force range, around 150 pN,

allowing them to obtain the full DNA stretching curve similar to the one seen in our experiments[33].

DNA Stretching Curve

The typical DNA stretching curve is obtained by stretching and releasing a single DNA molecule and plotting the force experienced by the DNA as a function of extension (Figure 12). This curve has been broken down into four-major sections[34,35] which are color coded in figure 12.

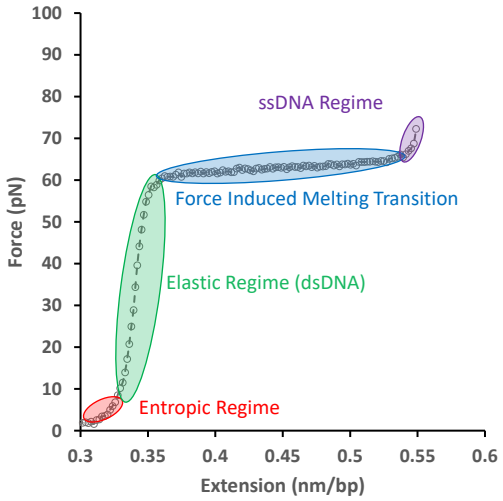

Figure 12: Force (pN) vs Extension (nm/bp) graph obtained during the stretching of DNA. The stretching curve has four distinct regimes highlighted with different colors.

The first section highlighted in light red is called the entropic regime. One can see that in this regime not much force is required for DNA extension, this is due to the fact that the DNA is originally slack, and it is stretched to be taught. Once taught the elastic regime begins, highlighted in light green. As the name indicates once the DNA is taught it begins to act as an elastic where more force is required for a small amount of extension. When the elastic regime hits around

65 piconewtons (pN) of force its believed that the DNA base pairs begin to separate, this is known as DNA melting, due to this structural change a substantial amount of extension can be seen with minimal force required, shown in blue. This region is known as the force induced melting transition. At the end of this transition most of the DNA base pairs have separated besides some Guanine, Cytosine rich regions that hold the two strands of melted DNA together. The two parallel single-stranded DNAs (ssDNA), once again act as an elastic. This region is called the ssDNA regime shown in purple. If too much force is applied here the last few base pairs that hold the two ssDNA will break and the strands will completely come apart.

Since the first stretching of the DNA, for more than a decade, scientist were divided on what is happening in the plateau region[36]. One group believed the DNA is transformed into a new form called s-DNA[37-39] and the other group believed it was a force induced melting of the dsDNA into two mostly ssDNA[33,40,41]. Combining florescents with optical tweezers (now known as fleezers) resolved this issue to our todays understanding[42]. The DNA stretching and the explanation of what's happening now have been accepted universally and are used as a base line to study the interactions of proteins and small molecules that bind to DNA. The BSU SMB lab mainly study small molecules that are either anticancer drugs or prospective anticancer drugs. As mentioned earlier, we believe that the anticancer drug BI-3802 investigated in this study looks similar to the special category of small molecules known as intercalators. Therefore, it is important to review how DNA stretching curves are altered in the presence of these intercalators.

Intercalating Drugs in Optical Tweezers Experiments

The majority of the drugs we study in the BSU SMB Lab are of a certain chemical structure called intercalators. Like briefly mentioned in the BI-3802 section intercalators have a flat planar section that stacks in between the DNA base pairs (Figure 13).

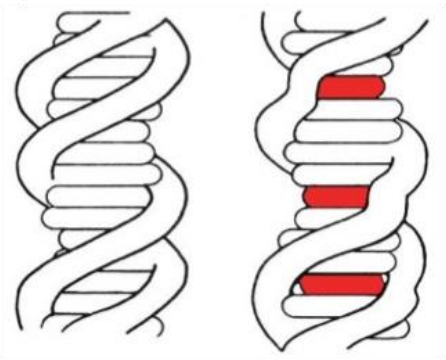

Figure 13: Cartoon representation of dsDNA (left) and intercalators (red) stacked between the DNA base pairs (right)

Intercalators are a very common form of anticancer drug due to this chemical structure. As previously stated, cancer is a disease caused by uncontrollable replication of certain cells. Intercalating drugs aim to slow or stop this rapid replication by stabilizing the double stranded structure of DNA. By stacking in between the DNA base pairs intercalators strengthen the double stranded structure of DNA preventing the separation of DNA strands necessary for cell replication. When the intercalating drugs stack in between the base pairs they also lengthen the DNA as can be seen in Figure 13, these effects were clearly observed in optical tweezers experiments.

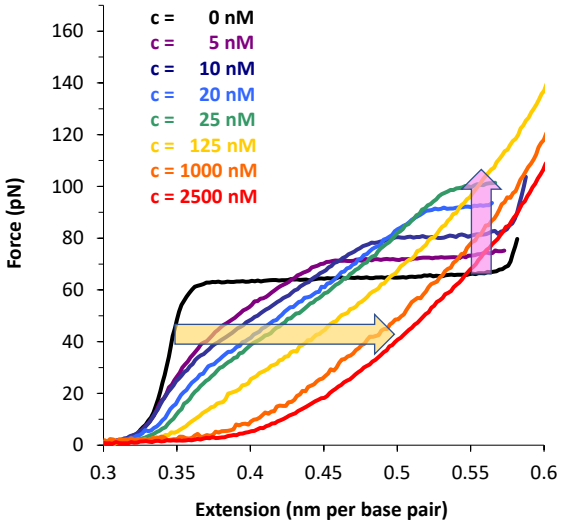

Figure 14: Force versus extension graph showing the effects of DNA stretched in the presence of seven different concentrations of the intercalating drug Ethereum bromide compared with DNA stretch with no drug present. A yellow arrow shows the increase of DNA length as the drug concentration increases. The pink arrow shows the increase of force required to melt the dsDNA as the drug concentration is increased.

Figure 14 features a force versus extension graph of DNA stretched in the presence of a common intercalating drug Ethereum bromide[43]. The effects of an intercalating drug on the structure of dsDNA can clearly be observed in this figure. The yellow arrow (around 40 pN) shows that as the concentration of the drug is increased the length of the dsDNA also increases. This is due to the drug stacking in between the dsDNA base pairs and physically lengthening the DNA. The more drug molecules stacked in between base pairs the longer the dsDNA structure becomes. This lengthening also increases with the increase in force as the force facilitates more intercalators to bind. The pink arrow points out that as the drug concentration is increased the force required to melt the dsDNA is also increased. As mentioned earlier the melting transition is where the dsDNA base pairs begin to open up, so the binding of the drug is preventing this separation from

occurring. This shows that the intercalators stabilize the dsDNA. At 1000 nM concentration (light orange curve) the DNA stretch does not exhibit melting transition indicating that the drug does not allow the base pairs to separate. Our hypothesis is that if BI-3802 is an intercalator it should exhibit these effects when stretching DNA in its presence.

Materials and Methods

Preparation of Biomaterials

Our experiments require four main biomaterials: buffer, polystyrene beads, DNA, and our prospective drug BI–3802. Buffer is the central most important biomaterial in our lab since it is the base of all our other biomaterials. In the SMB lab the buffer made is designed to imitate the physiological conditions of the fluid inside of a human cell. It is created by making a solution of 990 milliliters (ml) of a heavily filtered and deionized water called Milli-Q water, 10 ml of 1 M Tris (Ambion, AM9856) which is used to maintain the solutions pH, and 5.885 grams of sodium chloride (Sigma-Aldrich, S3014). The solution is then filtered using a Corning™ filter system (Fisher Scientific, 430515) and tested using pH strips to confirm a pH of 8. The final buffer solution is designed to have a salt concentration of 100 millimolar (mM). The buffer is stored in a sterile 1 L plastic container at room temperature.

The second biomaterial is the polystyrene beads (Spherotech, SVP-30-5) that are trapped with lasers. The beads are coated with a chemical called streptavidin and have a diameter of between 3.0 – 3.4 micrometers. The streptavidin allows for a link between the bead and the DNA which will be further discussed later in this thesis.

The third biomaterial is the DNA, which is from a bacterial virus called lambda phage, it is a classic model system for studying the physical nature of DNA[44]. The lambda phage DNA (Sigma-Aldrich, 10745782001), biotinylated nucleotides A and C (Thermofisher Scientific, 19518018, 19524016) and unlabeled nucleotides (Thermofisher Scientific, R0181) were purchased to label both three

prime ends of the DNA with a chemical called biotin. Then a gel extraction kit (Qiagen, 20021) was used to extract the DNA fragments in order to isolate the biotin labeled lambda DNA that is used in our experiments. The chemicals biotin and streptavidin have a very strong binding affinity with one another. This affinity allows the biotin on the ends of the DNA to attach to the coating of streptavidin on the beads, allowing us to isolate a single DNA molecule between two beads in our research. The DNA and beads are stored in a temperature-controlled refrigerator at 4 degrees Celsius (°C).

Our last biomaterial is the drug under investigation, BI-3802. BI-3802 was purchased (Med Chem Express, HY-108705) in liquid form (1 ml) at a concentration of 10 millimolar (mM). The drug was received emersed in liquid nitrogen to keep it frozen. Upon reception, the drug is allowed to thaw in the lab refrigerator. Once thawed it was vortexed to evenly mix the solution and then aliquoted into ten Eppendorf tubes. In each tube a stock solution of 100 μM was created by adding 998 micro liters (μl) of buffer and 2 μl of the 10 mM BI-3802. The BI-3802 stock solutions are stored in a -80 °C freezer. During experiments one of these stock solutions is step thawed by moving it to a -20 °C freezer for 2 hours, then a 4 °C refrigerator for 2 hours, and lastly it is kept at room temperature until fully thawed. The thawed solution is then vortexed to assure the solution is properly resuspended. This solution can then be added with buffer for a total 2ml volume solution, the volume of stock used is dependent on the desired concentration.

These biomaterials are repeatedly used in our optical tweezers experiments to study the interactions of the desired drug with DNA at the single molecule level. To understand how a single DNA molecule can be isolated for our experiments it is first necessary to comprehend the design of our optical tweezers setup.

Dual Beam Optical Tweezers Setup

The optical tweezers setup in the SMB lab at BSU is believed to be the first dual beam optical tweezers setup fully built and maintained by undergraduate students. The setup is constructed atop an air supplied levitating optical table. This is a key feature as it allows for minimal vibrational effects from the outside environment, a necessary feature since as mentioned in the introduction, extremely small forces are measured in the order of piconewtons (pN) during our experiments. A component diagram of the dual beam optical tweezers setup can be seen in (Figure 15)[45].

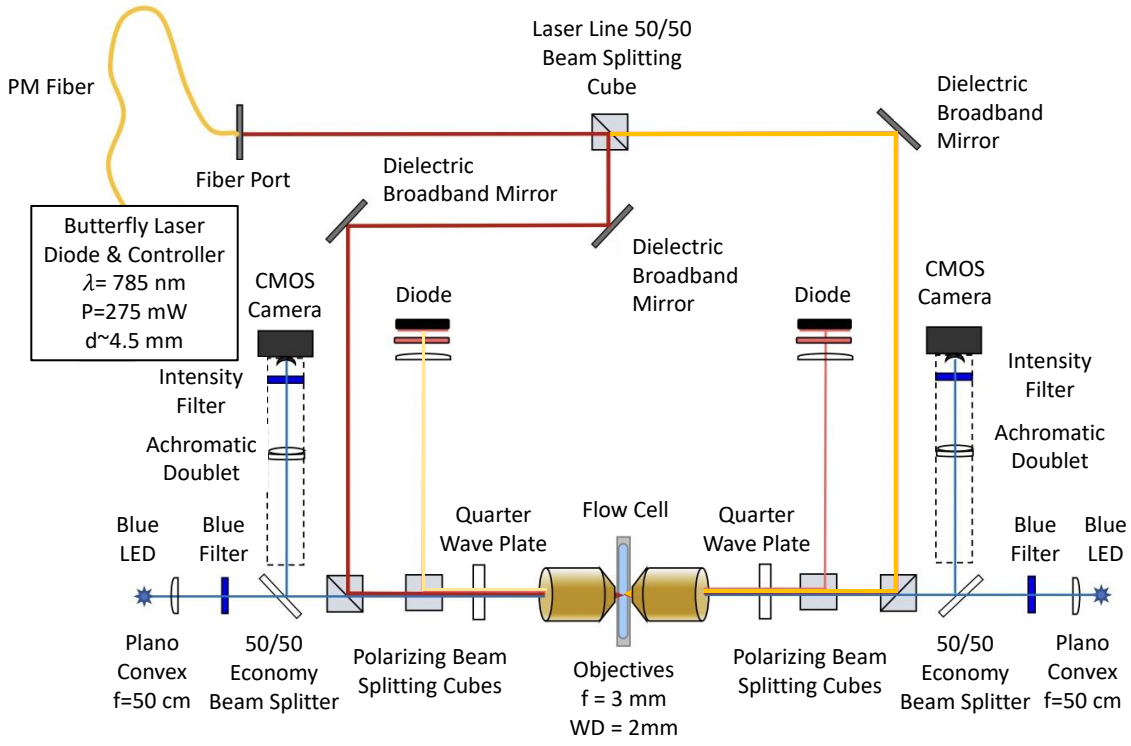

Figure 15: Component diagram of the dual beam optical tweezers setup in the Single Molecule Biophysics lab at Bridgewater State University.

The first component in the set-up is a temperature control box for the laser (Figure 16). The control box houses a custom-built butterfly laser diode (Lumics, LU0786M250). The laser diode has an operating power of 250 milliwatts which enables it to produce a 785 nanometer linearly polarized beam. The control box keeps the laser at its working temperature of 25 °C. This laser is then coupled to a polarization maintaining (PM) pigtail optical fiber cable. This cable guides the linearly polarized light to another coupling with an aspheric fiber port. The fiber port provides us with a columnated beam and can be adjusted so the light is linearly polarized perpendicular to the table. The columnated beam is now directed into a laser line 50/50 beam splitter cube, splitting the beam into two paths of equal power. These two paths have been highlighted in different colors (orange and red) for explanatory purposes.

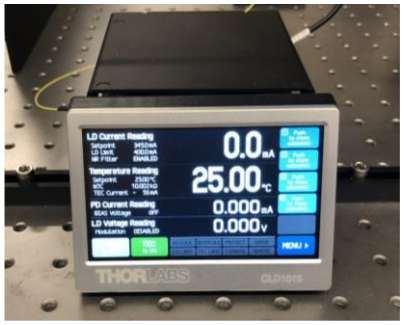

Figure 16: Image of the Temperature and Electrical control box used to house the diode laser in optical tweezers setup. It is set to hold the temperature at 25 ℃, the working temperature of the diode laser used.

Following the orange path, the beam next hits a dielectric broadband mirror reflecting the path at a 90-degree angle. This mirror is coated to minimize the loss of power specifically for wavelengths from 750 to 1100 nanometers. The mirror directs the light into a polarizing beam splitting cube which acts like a one-way mirror for our linearly polarized beam. The beam then hits another polarizing beam splitting cube, this cubes orientation allows for the beam, that is linearly polarized perpendicular to the table, to be transmitted through. The beam then goes through a quarter wave plate which changes the beam to become circularly polarized, a feature that becomes important for detection. Now, the beam enters the next element, the microscopic objective. The objective focuses the beam inside the flow-cell, a custom-made chamber where

our experiments take place. The microscopic objectives used have 60X magnification with a working distance (WD) of 2 mm. This completes the first side of our dual beam trap.

Following the red path, after exiting the 50/50 beam splitter, the beam hits one dielectric broadband mirror directing it towards another dielectric broadband mirror which directs the beam towards the polarizing beam splitting cube. From there, the beam takes a mirrored route from the orange path hitting the second polarizing beam splitting cube, quarter wave plate, and lastly microscopic objective focusing it inside the flow-cell. The two beams are aligned to have overlapped focal points inside the flow-cell creating our optical trap. For this to happen the beams had to be finely aligned going through every individual optical component.

Now with finely aligned lasers it is possible to trap the polystyrene beads. When a bead is caught in the trap, the beam from either side passes through the bead as well as the objective on the other side, which re-collimates the beam. When forces are exerted on the bead it will become slightly displaced which in turn causes a deflection in the laser beam. By steering this re-collimated deflected beam into a position sensing photo diode, these deflections can be measured and then converted into force measurements.

Let's see how the optical components are able to steer this light towards the detector. Each path is the same for detection, so let's just look at one, the orange path. The detection system is positioned upwards above the table so that it does not interfere with trapping or imaging (Figure 17). Therefore, in order to navigate the beam upwards polarizing beam splitting cubes are used. As mentioned earlier once the orange path hits the quarter wave plate the beam that is linearly polarized perpendicular to the table becomes circularly polarized. This beam next passes through both objectives being recollimated on the other side. The recollimated beam now enters through another quarter wave plate. This quarter wave plate turns the circularly polarized light back into linearly polarized light but this time parallel to the table. With this new polarization when the light hits the polarizing beam splitting cube it is reflected upwards towards the detector. A small amount of transient light is not deflected upwards and will be used during imaging. The optics used to direct the upward reflected light towards the detector are all positioned on a post connected to the table. The first component on the post is a plano convex lens. This lens focuses the light into the detector. A neutral density filter is placed directly before the position sensing diode in order to protect it from damage due to high power. The diode will detect this light and create a voltage dependent on the position of the laser spot which is then calibrated into position.

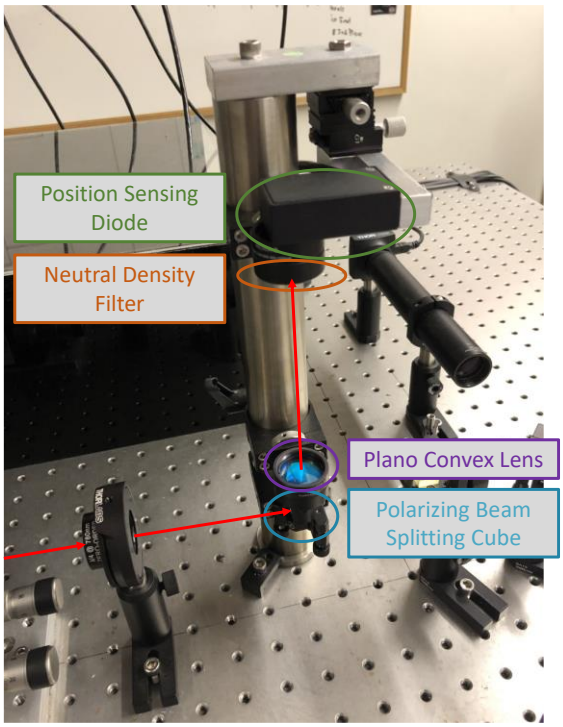

Figure 17: Image of the post used to house the components used for detection above the table. Each component is highlighted with a colored circled and a corresponding-colored caption. The laser path is represented with red arrows.

With the diode calibrated, any deflected lights position can be detected and converted into a force measurement.

Another important feature of the optical tweezers setup is imaging. It is crucial for us to have an image of inside the flow-cell chamber to properly conduct any experiment. A blue LED is used on either side of the set-up and its light is directed into a 50-mm focal length convex lens to collimate the light. This light now enters a 50/50 economy beam splitter which lets the light pass through from the rear side (this mirror reflects the light hitting from the front side). Since this blue light is unpolarized it passes through all of the following optical components unfazed until it hits the 50/50 economy beam splitter on the other side. Since the light now hits the front surface of the 50/50 economy beam splitter, it reflects the light towards the CMOS camera. The transient light from the laser is also reflected towards the camera along with the blue light. The light is focused on the camera using an acoustic doublet with a focal length of 200 millimeters and antireflection coating of 400 to 700 nanometers. A band pass filter is connected to the camera to protect it from excess laser exposure. The light hitting the cameras now gives us the image in Figure 18.

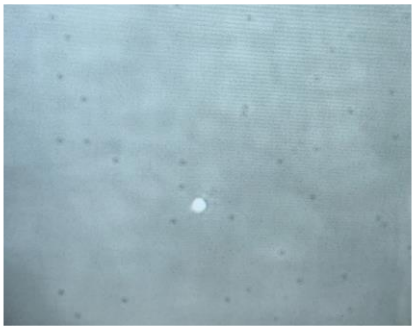

Figure 18: Image of the laser dot displayed on the monitor by the CMOS camera.

Flow-Cell Design and Creation

A flow-cell is a custom-made plexiglass microfluidic chamber were all our experiments take place. The making of a flow-cell starts with a 22 x 30 mm sized piece cut from a plexiglass sheet that is

2.4 mm thick (McMaster-Carr, 8589K32). This plexiglass piece is then precisely cut using a laser cutter in our machine shop on campus. The machine shop cuts the main channel in the plexiglass and drills three canals from the outside of the spacer into the channel, two canals on either side of the channel and one penetrating from the top. This results in a what is referred to as a flow-cell spacer (Figure 19).

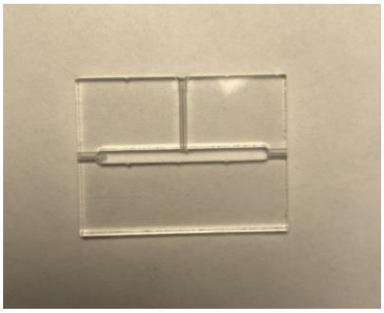

Figure 19: Image of the custom-made plexiglass flow-cell spacer featuring the main channel and three canals.

Upon receiving these spacers from the machine shop, their hole diameters are tested, and any loose plexiglass particles are removed. The machine shop uses oil to prevent the plexiglass from overheating and cracking during drilling therefore, this oil must be removed before constructing the flow-cells. To remove the oil the flow-cell spacers are soaked in hot soapy water overnight then rinsed and dried the following day. Before construction of a flow-cell, the spacer is once again thoroughly cleaned with hot soapy water and rinsed. Additionally, methanol is squirted in all of the spacer's holes and surfaces (while wearing gloves to protect our skin contacting methanol directly). Now with an assuredly clean flow-cell spacer the first step of creation, sealing the flow-cell, can be started.

With a steady hand a microscope glass slide is used to spread an even layer of optical adhesive (Thorlabs., NOA68) along one side of the spacer while minding not to get any adhesive in the channel or holes. Then a clean 30 x 22 mm No. 1 microscope cover glass (Fisher Scientific, 12-545-AP) is placed evenly atop the adhesive side of spacer. Next, the quality of the seal is examined by confirming there is no adhesive inside the channel, and there are no pockets of air extending the channel that could lead to future contamination or leakage. A UV lamp is then used to cure

the adhesive and this process is repeated on the opposing side of the spacer, this effectively seals the flow-cell channel creating a chamber. Upon sealing both sides of the flow-cell a borosilicate glass micropipette (WPI, TIP1TW1) is inserted into the channel through the top canal. The tip of micropipette is one micrometer in diameter and will break upon almost any contact, so it requires extreme caution and patience to insert one successfully. A microscope at 100 times magnification is used to guide the glass micropipette tip through the top canal of the flow-cell, pushing it about a little less than halfway into the chamber. When this is accomplished, the optical adhesive is applied to seal the pipette at the start of the top canal and cure the adhesive using the UV lamp. A diamond scribe is used to break the micropipette tip leaving about one half of an inch protruding from the flow-cell. Next, a 15 cm segment of Tygon Microbore Tubing with inner diameter 0.050" and outer diameter 0.090" (Cole Parmer, EW-06419-01) is cut off and fit it over the truncated end of the micropipette. Again, the adhesive is used to seal the tubing to the flow-cell.

The next step is to attach the inlet tubes. Four pieces of PE 10 tubing with inner diameter 0.011" and outer diameter 0.024" (VWR, 63019-004) is cut to be around 20 cm in length each. These tubing's are then taped together, and the ends are cut in order to align the four inlets. The aligned tubing's are then inserted into one of the flow-cells side canals such that they slightly emerge into the chamber. The inlet tubing's are sealed with adhesive. For our final tubing, the outlet tube which provides the outlet for the chamber, a 20 cm

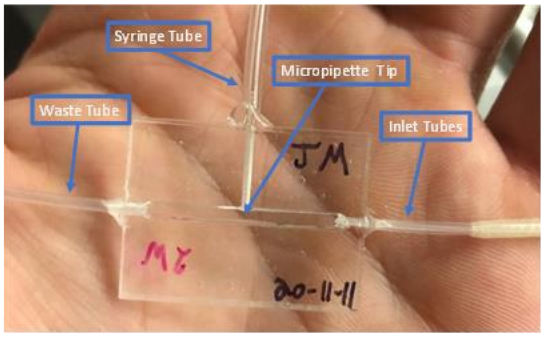

Figure 20: Image of a completed flow-cell. Captioned arrows point out the main features of the flow-cell: the Inlet tubes (right), waste tube(left), syringe tube (top), and micropipette tip (middle).

segment of PE 160 tubing with inner diameter 0.045” and outer diameter 0.062” (VWR, 63019-128) is cut and inserted it into the other side canal and sealed with adhesive. After around a 4-hour process, due to the curing time of the adhesive, results in the completed flow-cell (Figure 20). The next step is to properly place this flow-cell within our optical tweezers setup.

Setting Up the Flow-Cell for Optical Tweezers Experiment

When we are ready to start our experiments the first thing needed to be done is to attach the flow-cell to the optical tweezers. The first part of setting up the flow-cell is connecting the tubing’s. Our Biomaterials (buffer, beads, DNA, and drug) are held in four separate reservoir tubes that are attached to a custom-made housing (Figure 21).

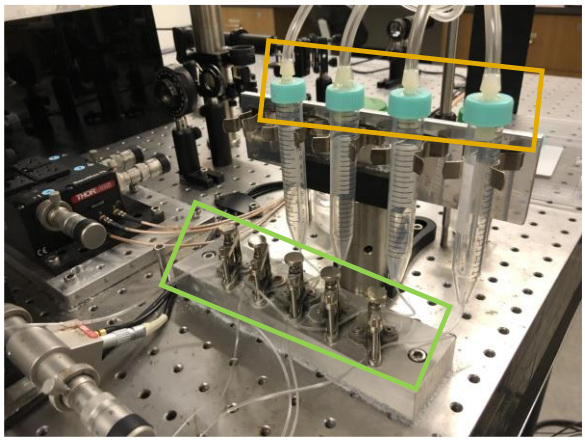

Figure 21: Image of the custom-made reservoir tube housing. The flow gates are outlined within a green box. The reservoir tube caps that are connected to the compressed air system are outlined within an orange box.

Each reservoir tube is labeled a separate biomaterial and each reservoir has its own tubing. Each tubing goes through a key feature of the custom-made housing, a mechanical press referred to as a flow gate (outlined within the green box in Figure 21), it has the capability to pinch the tubing’s closed in order to prevent backflow of biomaterials from the flow-cell. With the flow-cell inlets labeled each inlet tube is attached to its corresponding reservoir tubing by simply slipping the inlet tubing inside that of the reservoir (it is a tight seal). The lid caps of the reservoir tubes are connected to a compressed air system (outlined within orange box in Figure 21).

This air system creates a pressure to flow the biomaterials into the flow-cell through a relay system. The relay system gates are controlled using a custom-made electrical flow control box (Figure 22). This control box allows us to switch between different biomaterial flows that enter the flow-cell.

Figure 22: Image of the custom-made electrical flow box that controls the flow of each biomaterial (Buffer, Bead, DNA, and Drug) with its own switch.

All the waste from our experiments is collected in a waste container through the outlet tubing. The waste container features a screw cap with a tubing going through the middle of the cap (Figure 23). The outlet tubing from our flow-cell is slipped inside the tubing from the top of waste container to complete that seal, this tubing also goes through a flow control gate. Lastly, the syringe tubing, the tubing on top of the flow-cell attached to the glass micropipette inside the flow-cell, is connected. The end of this tubing is connected to a syringe. The syringe now gives us the ability to inject or retract air from the system through the micropipette. This is a key feature for conducting experiments and for cleaning of the flow-cell.

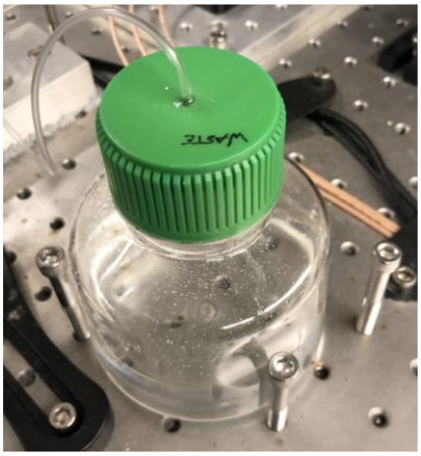

Figure 23: Image of the waste container where all the biomaterials used during experiments are collected after flowing through the flow-cell.

Testing the Flow-Cell

With the flow-cell now attached its adequacy in performing experiments is checked. First, around 2 ml of buffer is added into each reservoir tube, the caps are attached, and the flow is started in one reservoir. All flow gates are kept closed besides the one that controls the flow from the reservoir tube that is flowing and the waste container. This test is done to confirm the tubing is not clogged and there are no leaks in the tubing or seals. This also cleans the tubing and flow-cell chamber of any dust or small debris. This step is repeated for all four reservoir tubes. Once the whole buffer is flowed through the system a small amount of buffer is added to each reservoir tube and allowed to flow through the tubing in order to fill in the tubing and keep air bubbles out of the system. The next adequacy test for the flow-cell is confirmation of a working micropipette tip. It is not uncommon that a micropipette tip is unknowingly broken or that the micropipette became clogged by adhesive or glass shards. The micropipette tip is tested for clogs during the reservoir cleaning process explained above, by pushing the plunger of the syringe to see if there are air bubbles coming from the micropipette tip. A flow-cell with a clogged micropipette tip cannot be used for experiments. With that test passing the next test is to check for cracks/breaks in the micropipette tip. To do this the optical tweezers setup must be used to obtain an image of the micropipette tip.

The flow-cell is carefully docked in between the objectives on a holder (Figure 24) which is housed on a piezoelectric controlled stage. The piezoelectric controlled stage allows for three axes of small, controlled movements of the flow-cell. The stage features manual controls (Figure 24) for course and fine movements. The temperature control box of the laser is turned on and left to reach the working environment temperature of 25 °C before turning on the laser. Deionized water is squirted on both sides of the flow-cell in order to make a continuous medium between the objective and the flow-cell. Then, one of the blue LEDs and the corresponding camera are turned on to obtain an image of inside the flow-cell. This image is projected to a monitor that is connected to a camera, which is housed on a ceiling mounted rack above the optical tweezers.

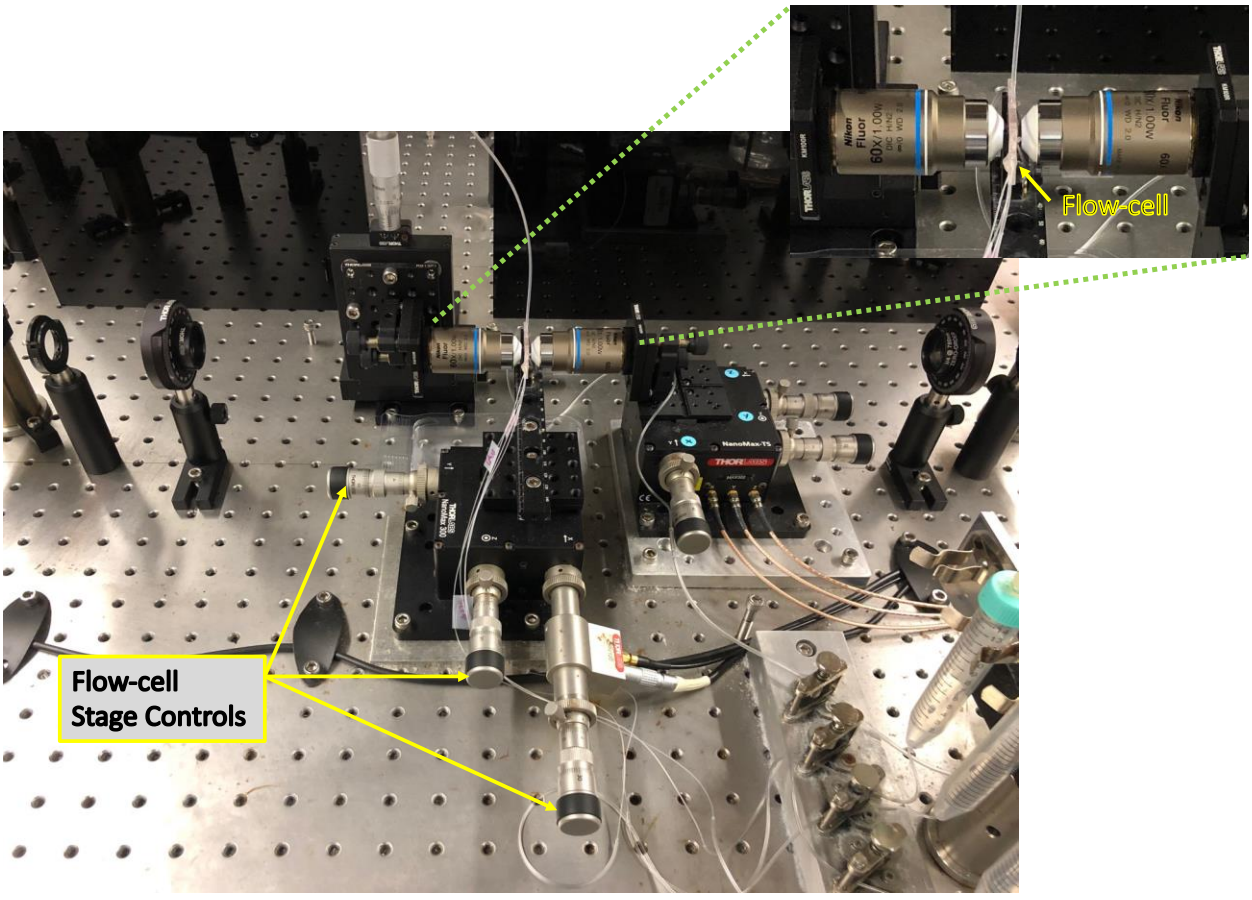

Figure 24: Image of the x, y, and z axis manual controllers for the flow-cell stage (bottom left) as well as a zoomed in image of the flow-cell docked in between the two objectives (top right).

Now, the cameras are used to obtain an image of inside the flow-cell and to find the micropipette tip. First, it is confirmed that the camera is looking through the chamber of the flow-cell (the only place an image can be obtained). Next, the piezoelectric controls are used to move our flow-cell and bring our image to the top of the flow-cell chamber, this will be the easiest place to find the micropipette as its at its thickest. We know we are at the top of the chamber when the image begins to darken as this means we are getting close to changing mediums. While at the top of the chamber the flow-cell is moved back and forth carefully by hand while watching the screen, looking for the unfocused micropipette. Once the dark blurry image of the micropipette is found the piezoelectric controls are used to move down towards its tip while at the same time controlling the focus (z axis) as to not lose the image. By following the micropipette image downwards, the image of the tip is obtained. With this image the tip can be examined for any breaks, an example of a broken tip can be seen in Figure 25. Both the tip and laser dot are 1 micron in diameter but in this image, it can be seen that the tip is larger than the dot suggesting the tip is broken.

Figure 25: Screenshot of a broken micropipette tip imaged inside a flow-cell

A flow-cell with a broken micropipette tip is unusable because it cannot be used for proper sealing to attach beads (This will be discussed later).

Once the flow-cell chamber is cleaned, and it is checked for clogs in the tubing, any leakage in the flow-cell system and for an unbroken tip with no clogs the setup of the flow-cell is complete. The daily alignment of the optical tweezers now can be started.

Basic Laser Alignment

At the beginning of every day of experiments the optical tweezers need a small alignment in order to perform to the best of their ability. A sequence of small adjustments is made to finely align the counterpropagating beams of the optical tweezers. As discussed in the dual beam optical tweezers setup section earlier the lasers are detected with a pair of position sensing diodes after going through the flow-cell. The first step of our alignment is to manually move the position sensing diodes to have the laser focused on the middle of these sensors. This is done by adjusting the two-dimensional stage to which the sensors are attached. This process is guided with the help of a computer program that projects the position of the laser spots as dots (green and blue indicates the detectors on either side) in a coordinate system (Figure 26A). The sensor stages are adjusted in order to bring both sensor dots to the middle of this graph as can be seen in Figure 26B.

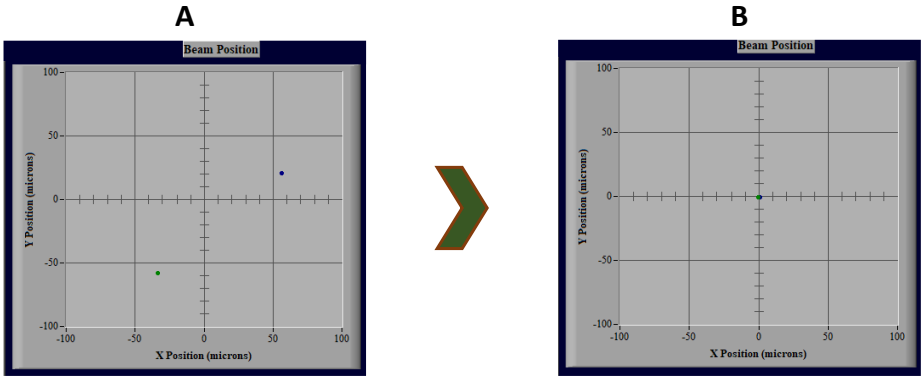

Figure 26: Screenshots of the computer program used to align the position sensing diodes (PSD). (A) Green and blue dots each representing a PSD are not at the origin of the graph indicating that PSDs are not positioned to have the laser spots to hit at their center(B) Both the green and blue dot at the graph's origin indicating that the laser spot is now hitting center of the PSDs.

Next, the right camera and its corresponding LED are turned on. Looking at the image from the right camera the micropipette is moved (by moving the stage) just above the laser dot. Then the imaging is switched to the left camera. If the micropipette is not just above the laser dot as seen with the first camera, the piezoelectric controls of the objective stage are used to move the objective to bring the laser dot to the same spot as the first image. The viewing is switched between cameras and these steps are repeated until the images are identical and the detectors remain aligned.

Obtaining the Trap Stiffness

Now that the basic alignment has been completed the last checkpoint before starting our experiments is to obtain the trap stiffness. Trap stiffness is a measure of how "stiff" our optical trap is or in other words the strength of the trap's alignment. To obtain the trap stiffness it is necessary to first trap a polystyrene bead. Protective latex gloves are worn as streptavidin is hazardous chemical, with gloves on we can then get the beads from the refrigerator. As can be seen in Figure 27A the beads will be resting at the bottom of the solution, so a vortex is used to suspend the beads creating the cloudy solution in Figure 27B.

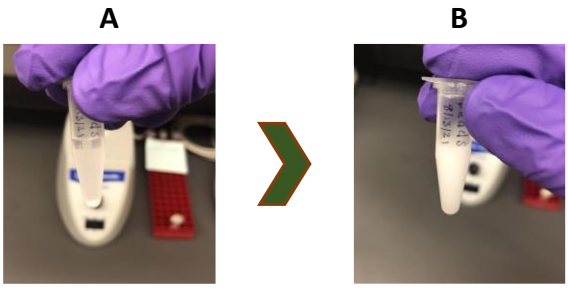

Figure 27: The state of polystyrene beads in a vial before and after being mixed with a vortex machine. (A) The beads clustered at the bottom of the vial with a slightly cloudy solution above before vortexing. (B) A fully clouded solution with the beads evenly suspended throughout the vial after vortexing.

Nearly 2 ml of buffer is added into the beads reservoir tube and 2 µl of beads is pipetted into the reservoir. This solution is vigorously mixed using the pipette by a continuous suction and release motion in order to evenly disperse the beads in the solution. Now the flow gate is opened and the switch on the flow control box is flipped to begin flowing our beads into the system. Once a bead is trapped by the laser (Figure 28A) the syringe is used to attach the bead to the micropipette through suction (Figure 28B). The beads flow is stopped and the excess beads inside the flow-cell are flushed out by flowing around 1 ml of buffer.

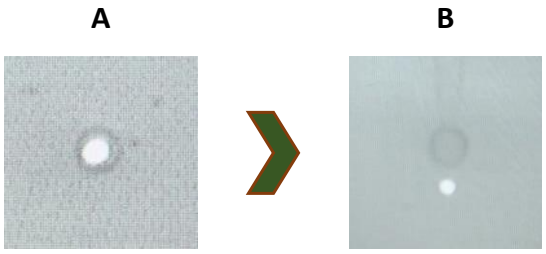

Figure 28: Attaching the bead to the Micropipette. (A) A polystyrene bead (grey) caught in the laser trap (bright white spot). (B) The bead after being suctioned to the micropipette tip.

Once the flow-cell chamber is cleaned the bead attached to the micropipette tip is manually moved just to the right of the laser dot. A custom-made computer program is then used to control the piezoelectric stage that holds the flow-cell, to move the bead to the left passing it through the trap, and then return to its original position. This program also collects the defection of the laser recorded by the position sensing diode to create a deflection (which is proportional to force) versus position graph (Figure 29). The readings from the two detectors are represented by the green and blue points in the graph. The solid circles represent the bead moving to the left through the trap and the open circles the bead moving right through

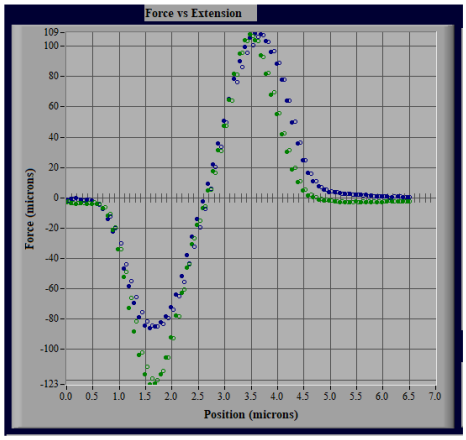

Figure 29: Screenshot of the Trap Stiffness. The deflection of laser detected by the detectors (blue and green representing PSDs on either side) as a function of position of the bead attached to the tip. The deflection is labeled as force since it is proportional to the force and used to calculate force in stretching experiments. The open dots are showing the return path.

the trap on the return. If the majority of the linear region in the middle of the graph (between the minimum and maximum deflection) from both detectors is aligned, then both lasers are properly aligned. The data obtained during the trap stiffness curve is saved as it will be used later for analysis.

Trapping and Stretching a Single DNA Molecule

Now with an optimized optical trap the experiments can be started. As mentioned in the introduction, in the BSU SMB lab optical tweezers are used to isolate single DNA molecules. A cartoon depiction of major steps in isolating a single DNA molecule is represented in Figure 30.

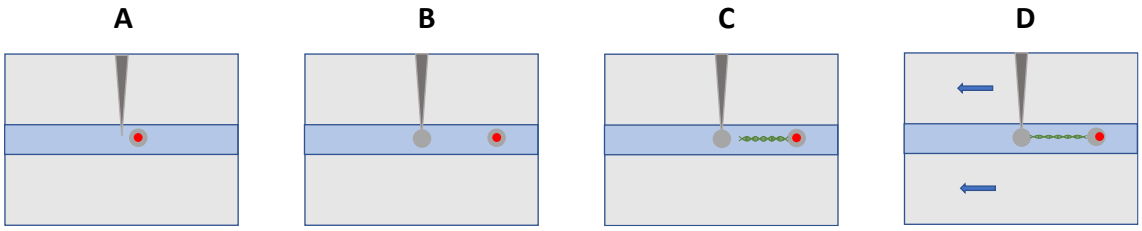

Figure 30: Cartoon representation of the major steps used to isolate a single DNA molecule using optical tweezers: (A) A bead trapped by laser (red dot), (B) Second bead trapped by laser after attaching the first bead to the micropipette (black), (C) One end of the DNA attached to the bead in the trap, (D) Other end of DNA attached to the bead held by the micropipette.

In order to catch a single DNA molecule, first two beads need to be trapped. As mentioned in the previous section the first bead is trapped (Figure 30A) and attached to the micropipette tip through suction while obtaining the trap stiffness. Once again, the beads are flown into the system and another bead is trapped by the laser (Figure 30B). After the second bead is trapped,

the excess beads are rinsed out of the flow-cell using 1 ml of buffer. The bead attached to tip is brought close (by moving the flow-cell manually) to the bead in the trap and tapped against it to make sure they are on the same plane. It is necessary to have the beads on the same plane to attach a single DNA molecule between them. If they are not in the same plane, the z axis of the stage that contains one of the objectives is adjusted slightly using the piezoelectric control. With two beads trapped and on the same plane a single dsDNA molecule can now be tethered between the beads.

The DNA must be handled carefully as it can easily clump together. The DNA reservoir is filled with nearly 2 ml of buffer, and 2 µl of DNA is gently pipetted into the reservoir tube. In order to suspend the DNA in the buffer, the solution in the reservoir is very slowly pipette mixed for about 5 or 6 times with a 1000 µl tip. Now DNA can be flowed into our system. As discussed in the introduction DNA molecules are on the nanometer scale, due to this size they will not be visible on our monitor image magnified by the microscopic objectives. Due to the Biotin-Streptavidin bond one end of the DNA will randomly attach to the bead in the trap and float with the flow (Figure 30C). The flow-cell stage controls are used manually to move the flow-cell (which in turn moves the micropipette) in an almost fly-fishing motion to catch the free-floating end of the DNA. If when the micropipette bead is moved to the left the bead in the trap also moves along with it, it is realized that a single DNA molecule is tethered between the beads (Figure 30D).

The next step is to stretch the DNA molecule and see if it is suitable for experimental use. To stretch the DNA, the same computer program that was used for obtaining the trap stiffness is again used. The program is run a couple of times and the number of steps is incrementally increased until all the DNA stretching regimes discussed in the introduction occur. If the stretch

and release overlaps without huge hysteresis and the melting transition is around 10 microns, it is a good DNA. If not, the DNA may be entangled or pre-melted, and the flow-cell has to be cleaned and the process should start from scratch trapping fresh beads.

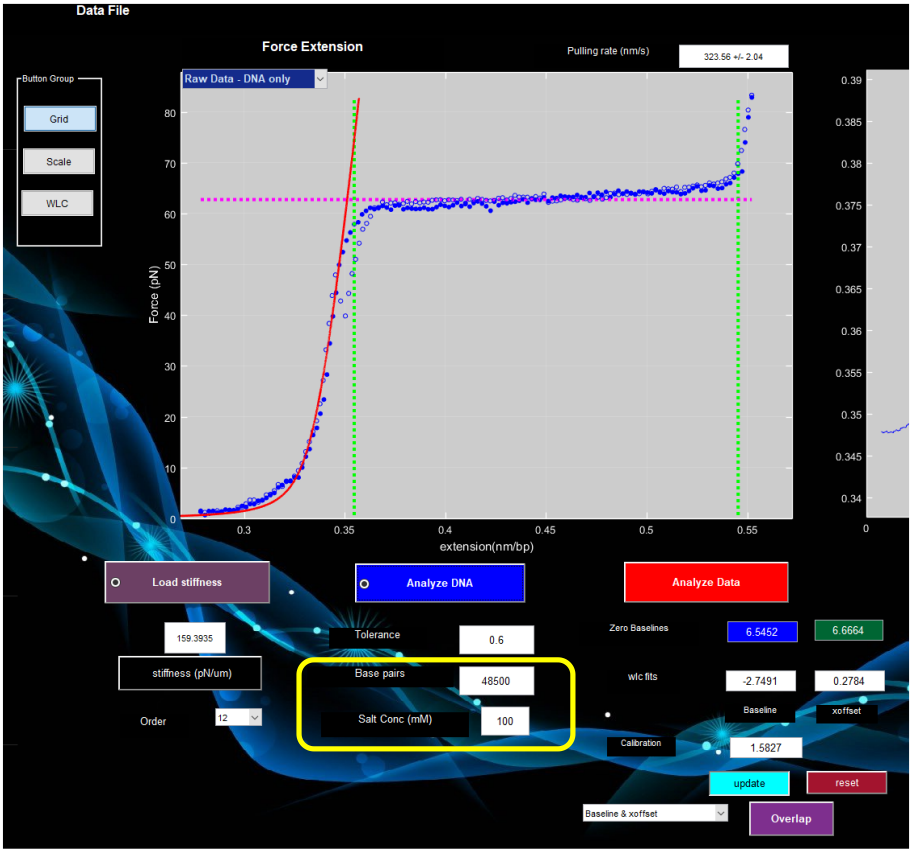

Figure 31: Screenshot of the program used to analyze DNA. The two parameters that must be adjusted (number of base pairs and salt concentration) are encapsulated in the yellow box. The image features an analyzed DNA that fits: worm like chain model that describes the dsDNA (red curve), melting transition force (pink broken line), and the beginning and ending of the melting transition (green broken lines).

Once a good DNA stretching curve is obtained, the data is saved and analyzed using the analysis program made by Northeastern University (Figure 31). The number of DNA base pairs is set to 45000 and the salt concentration is set to 100 mM (parameters encapsulated in yellow box in Figure 31). Then the trap stiffness file is loaded (purple button) and the analyze DNA button (blue)

is clicked to upload the DNA stretching data and analyze it. The DNA data will be compared to the polymer fitting model (WLC) to provide quantitative judgement if the DNA is suitable for experimental use. In general, the next step is to test the drug of interest by flowing the drug into the system and stretch the DNA again.

Control Experiments with DMSO

Our drug BI-3802 is dissolved in a solvent known as Dimethyl sulfoxide (DMSO). DMSO has a refractive index of 1.4768[46] while the refraction index of our buffer is around 1.335 (similar to water). This led us to believe that due to the change in refraction index at some buffer-DMSO ratio our trap stiffness would begin to be affected. Since DMSO based drugs had not yet been studied in our lab some preliminary tests using DMSO needed to be done before conducting the BI-3802 experiments. The goal of this preliminary test was to see whether there is any effect due to DMSO, and if there is any, what is the threshold that limits our experiments. The trap stiffness was obtained in the presence of five different volumes of DMSO added increasingly into 2 ml of buffer.

Previous studies have shown that DMSO has the ability to affect the double stranded structure of DNA[47]. Our goal was to find at what ratio of buffer-DMSO this would happen for our experiments. DNA molecules were stretched in the presence of four different volumes of DMSO added into 2 ml of buffer. This provided the ratio of buffer-DMSO that would affect the experiments and the limiting threshold for the experiments with BI-3802.

Experiments with BI-3802

To start the experiments with BI-2802, first different concentrations of BI-3802 were probed to find where the drug begins to have effects on the dsDNA stretching curve. To mix the drug with the buffer a combination of vortexing and vigorous pipette mixing was used. Around 1 ml of the drug solution is flowed into the system to where the flow-cell chamber is assuredly filled with just this solution. The DNA is then stretched, and the data is loaded into the analysis program, the analyzed data is saved. This allows for comparison of the original DNA stretch with no drug to the DNA stretched in the presence of the drug. The drug concentrations were started in the nM range as many of the previously studied intercalating drugs in our lab have shown effects at nM concentrations[28,29,31,48]. After no effects were seen in the nM range the concentrations of BI-3802 were increased until an effect was observed. The DNA stretch and release experiments were carried out at different concentrations of BI-3802 until we reached the threshold limited by the DMSO. At least three different DNA molecules were used to obtain three data sets at each concentration of BI-3802.

Results

It was a devoted effort to get to this part of the project. We ran into many pitfalls and footholds while conducting research and learned to overcome and learn from the mistakes made along the way. You learn to shake off the days where things are not cooperating which tend to be many and alternatively learn to use and abuse the days where things are running smoothly which tend to be far and few between. After months of planning, more months of learning techniques and creating flow-cells, and almost a year of conducting experiments we have collected data and compiled the following results.

Trap Stiffness in the Presence of DMSO

During our experiments the optical trap is aligned, and the trap stiffness curve is obtained using a buffer filled flow-cell before each experiment. As described in the methods section, this stiffness curve is used during the analysis of data. Our drug BI-3802 is dissolved in the solvent DMSO, which has a higher refractive index then that of our buffer. Therefore, after a certain volume of DMSO added into buffer the refractive index may increase enough to have an effect on the stiffness of our trap. It is important to figure out what level of DMSO can be added into the buffer without significantly affecting the stiffness curve. These were the first set of control experiments we performed.

Figure 32 below features the trap stiffness curve obtained without the addition of DMSO (black), which is used as the experimental baseline, along with the trap stiffness obtained in the presence of 1 µl (purple), 2 µl (blue), and 5 µl (green) DMSO added into 2 ml of buffer. Comparing the data, we can see that the linear region in the middle of this graph is unchanged for all the data sets. This allows us to conclude that the trap stiffness is unaffected up to 5 µl of DMSO added into 2 ml of buffer.

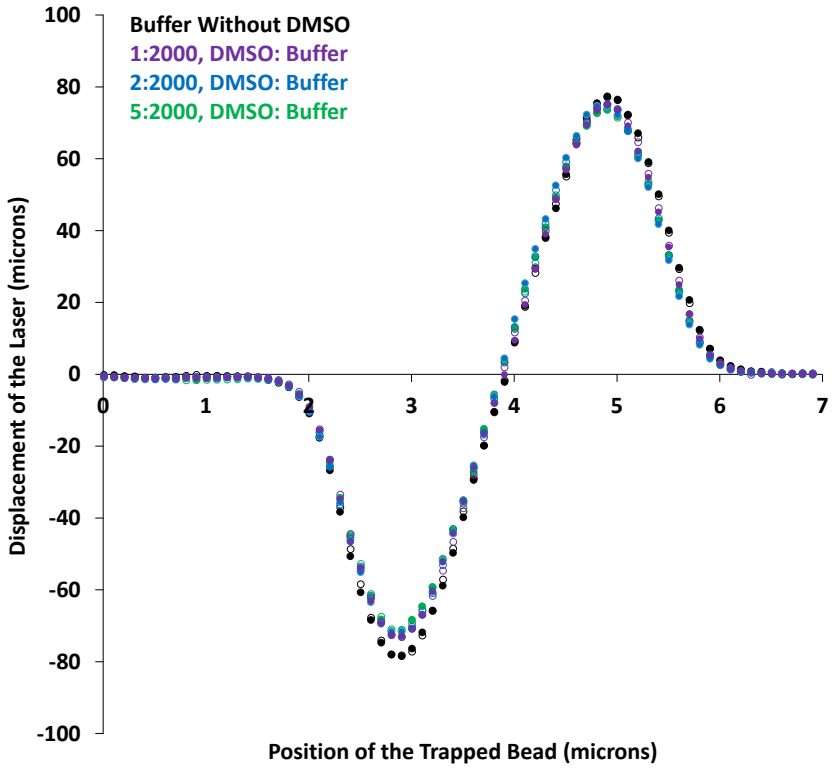

Figure 32: Trap stiffness without DMSO added (black) compared with the trap stiffness obtained in the presence of 1 µl (purple), 2 µl (blue), and 5 µl (green) of DMSO added into 2 ml buffer. The solid circles are deflections observed when the bead is moved from left to right through the laser trap and open circles are the deflections observed during the return to the original position.

We continued increasing the volume of DMSO added into 2 ml of buffer until an effect was observed. In Figure 33 we obtained the trap stiffness in the presence of 10 µl (yellow) and 20 µl (red) of DMSO added into 2 ml of buffer and again compared it to the trap stiffness obtained in the presence of buffer alone (black). Looking at the linear region in the middle of the graph an effect can be observed for both the yellow and red curves. This led us to the conclusion that going over the threshold of 5 µl of DMSO added into 2 ml of buffer has enough change on the refraction index of the medium to where our trap stiffness is affected.

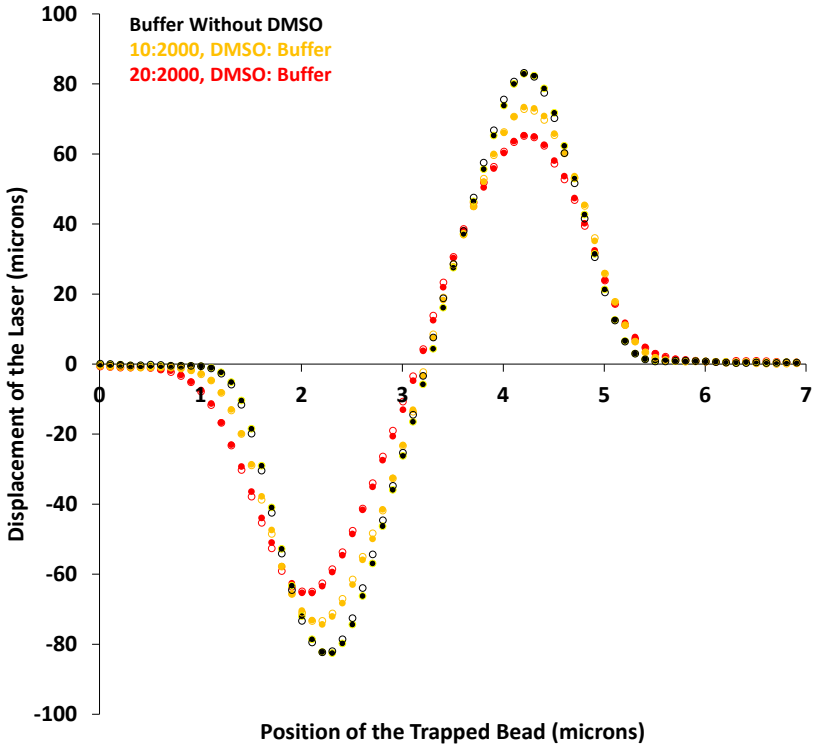

Figure 33: Trap stiffness without DMSO added (black) compared with the trap stiffness obtained in the presence of 10 µl (yellow) and 20 µl (red) of DMSO added into 2 ml buffer. The solid circles are deflections observed when the bead is moved from left to right through the laser trap and open circles are the deflections observed during the return to the original position

Stretching DNA in the Presence of DMSO

We also discussed in the methods section that previous studies have shown DMSO has the ability to affect the double stranded structure of DNA. We needed to be certain that effects seen in our BI-3802 experiments were due to the drug and not the solvent (DMSO). To have this certainty we performed a preliminary test to probe were DMSO has an effect on the stretching of DNA. Figure 34 shows the analyzed results from three different stretches of a single DNA molecule.

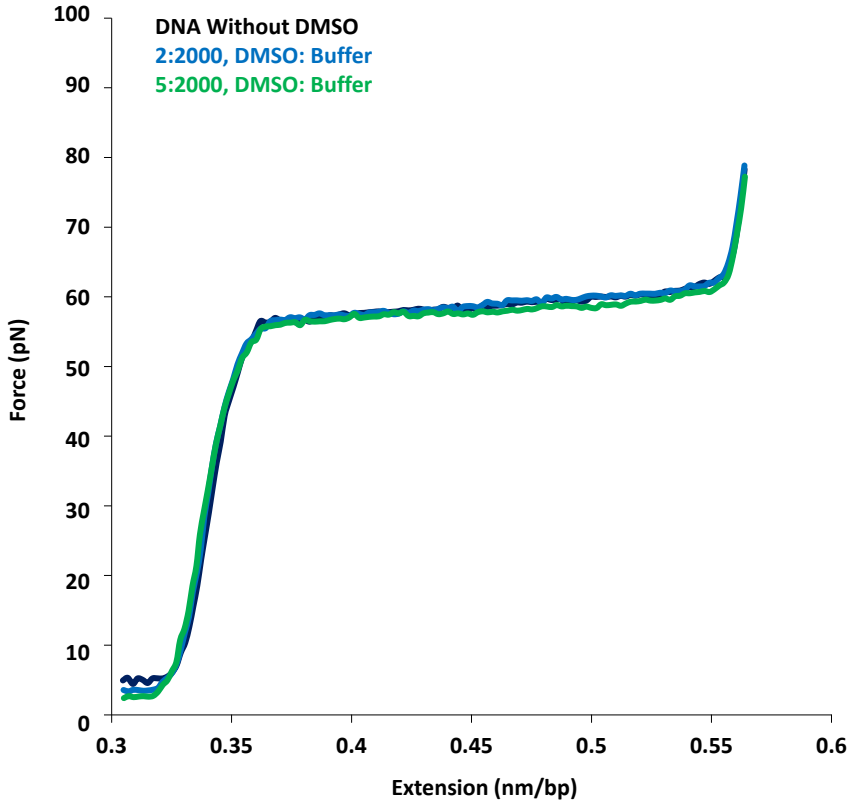

Figure 34: Force versus Extension graph displaying the stretching of a single DNA molecule without DMSO added (black curve) compared with the stretching of a single DNA molecule in the presence of 2 µl (blue curve) and 5 µl (green curve) of DMSO added into 2 ml of buffer.

The DNA was stretched in the presence of buffer alone (black curve), 2 µl of DMSO added into 2 ml buffer (blue curve), and 5 µl of DMSO added into 2 ml buffer (green curve). By observing the graph, it can be seen that the DNA stretching curve was unaffected at these volumes of DMSO. Like in the previous preliminary test, we continued increasing the volume of DMSO added into 2 ml of buffer until an effect was observed. Figure 35 illustrates a single DNA molecule stretched in the presence of 10 µl (orange curve) and 20 µl (red curve) of DMSO added into 2 ml buffer and again compared it to DNA stretched in the presence of the buffer alone (black curve).

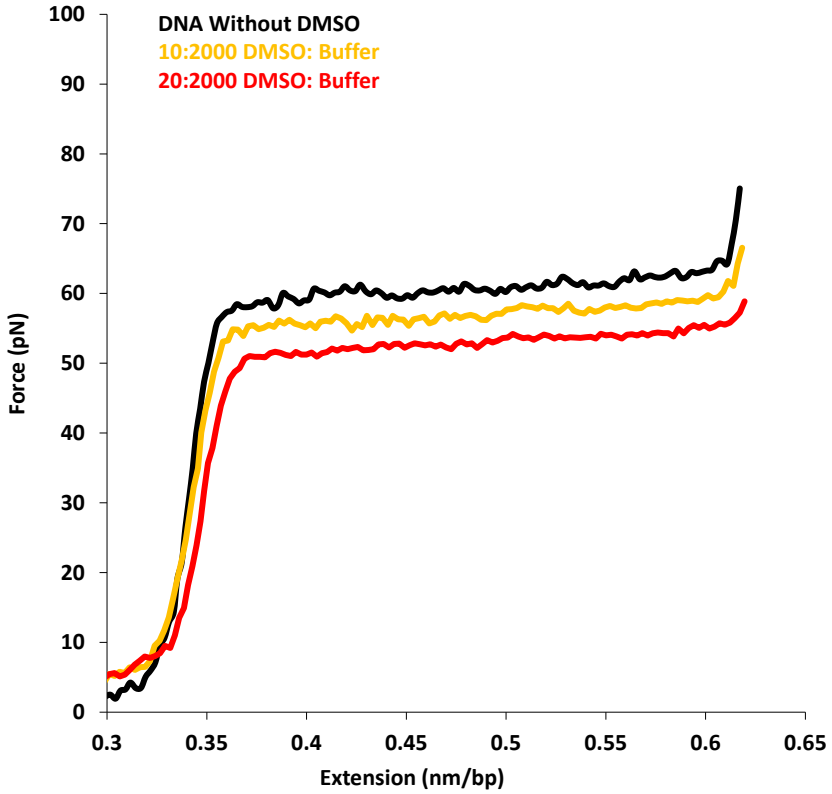

Figure 35: Force versus Extension graph displaying the stretching of a single DNA molecule without DMSO added (black curve) compared with the stretching of a single DNA molecule in the presence of 10 µl (blue curve) and 20 µl (green curve) of DMSO added into 2 ml buffer.

By observing the graph, it can be seen that with increased DMSO volumes the force required to melt the dsDNA is decreased. As mentioned in the introduction the melting transition is where the dsDNA base pairs begin to open up, so the DMSO is facilitating this separation. This shows that the DMSO destabilizes the structure of dsDNA, but these effects are not seen under the threshold of 5 µl of DMSO added into 2 ml of buffer. Based on these two preliminary tests we know if the drug solution is kept under the ratio 5 µl of DMSO added into 2 ml of buffer, our experiments will not be affected by DMSO.

Stretching DNA in the Presence of BI-3802

With the preliminary tests completed, we were able to begin investigating the interaction between BI-3802 and DNA. As mentioned in the methods section we started the drug investigations by probing nM concentrations of BI-3802 as many of the previously studied intercalating drugs in our lab have shown effects at nM concentrations. After no effects were seen in the nM range the concentration of BI-3802 was increased until an effect was observed.

The first effect was observed when DNA was stretched in the presence of 1 µM of BI-3802, this effect was proven to be repeatable. Figure 36 below shows the force vs extension graph for the DNA molecules stretched in the presence of 1 µM of BI-3802. Eight different single DNA molecules were stretched in the presence of 1 µM of BI-3802 (light blue curves) and were averaged to represent the effect (dark blue curve). Comparing this average to the DNA stretched in the presence of the buffer alone (black curve), a small decrease in the DNA melting transition force from 63±2 pN to 62±1 pN was observed in the presence of BI-3802.

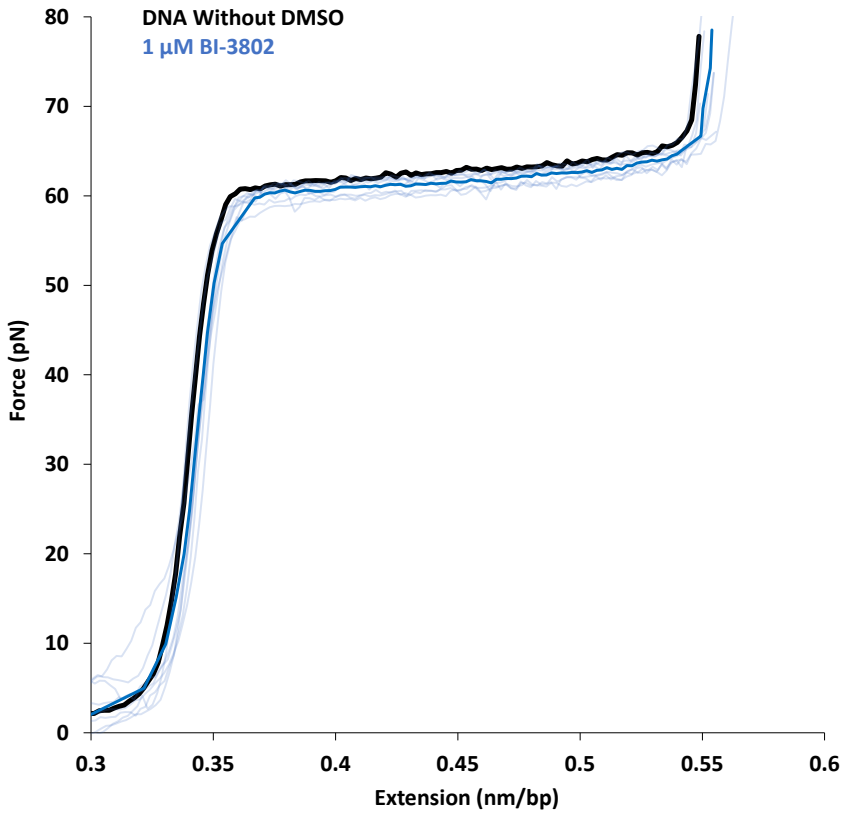

Figure 36: Force versus Extension graph displaying the stretching of a single DNA molecule without DMSO added (black curve) compared with the stretching of 8 separate DNA molecules in the presence of 1 µM BI-3802 (light blue curves) that are averaged into one curve (dark blue curve).

We then went on to collect data at our next increased concentration of BI-3802, 10 µM. Figure 37 features a force versus extension graph showing the stretching of 6 different single DNA molecules in the presence of 10 µM BI-3802 (light green curves); these were averaged together to show the ensemble average effect (dark green curve). When comparing this average to the DNA stretched in the presence of buffer alone (black curve), it continues the trend from the 1 µM stretches exhibiting a further decrease in the melting transition force to 60±2 pN in the presence of 10 µM BI-3802.

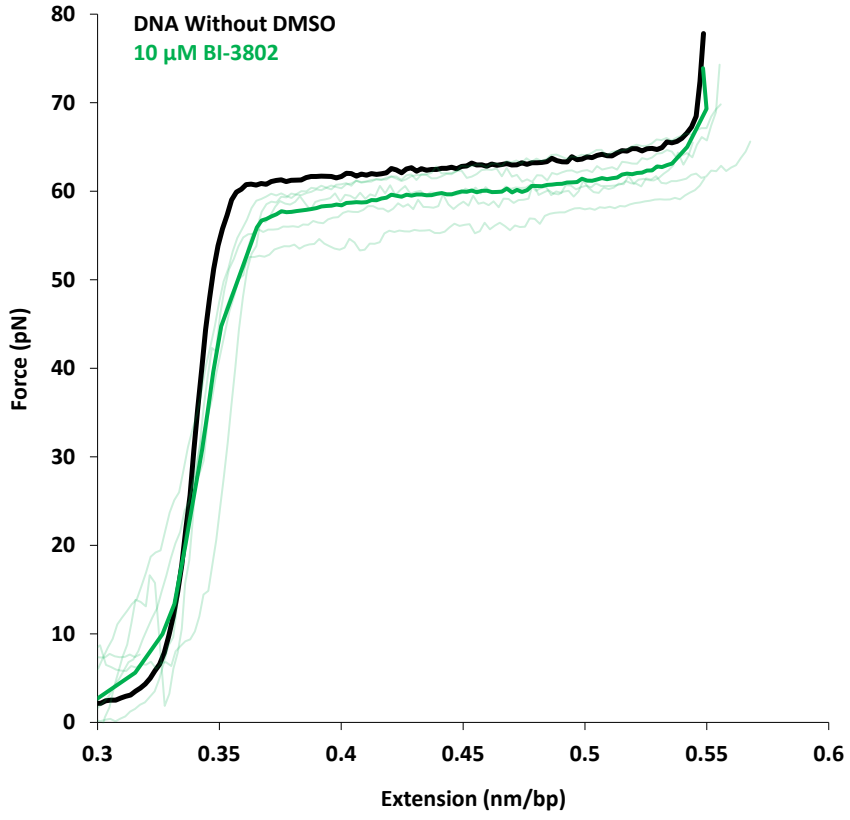

Figure 37: Force versus Extension graph displaying the stretching of a single DNA molecule without BI-3802 added (black curve) compared with the stretching of 6 separate DNA molecules in the presence of 10 µM ofBI-3802 (light green curves) that are averaged into one curve (dark green curve).

We next stretched DNA molecules in the presence of 50 µM BI-3802. This was the final concentration of BI-3802 in which we were able to collect data. Figure 38 shows the plotted data from the stretches of two different DNA molecules (light red curves) in the presence of 50 µM BI-3802. These stretches were averaged together (dark red curve) and compared to the DNA stretched in the presence of buffer alone (black curve). Again, lowering of the melting transition force to 56±2 pN in the DNA curve as well as continuing the trend from the 1 µM and 10 µM stretches.

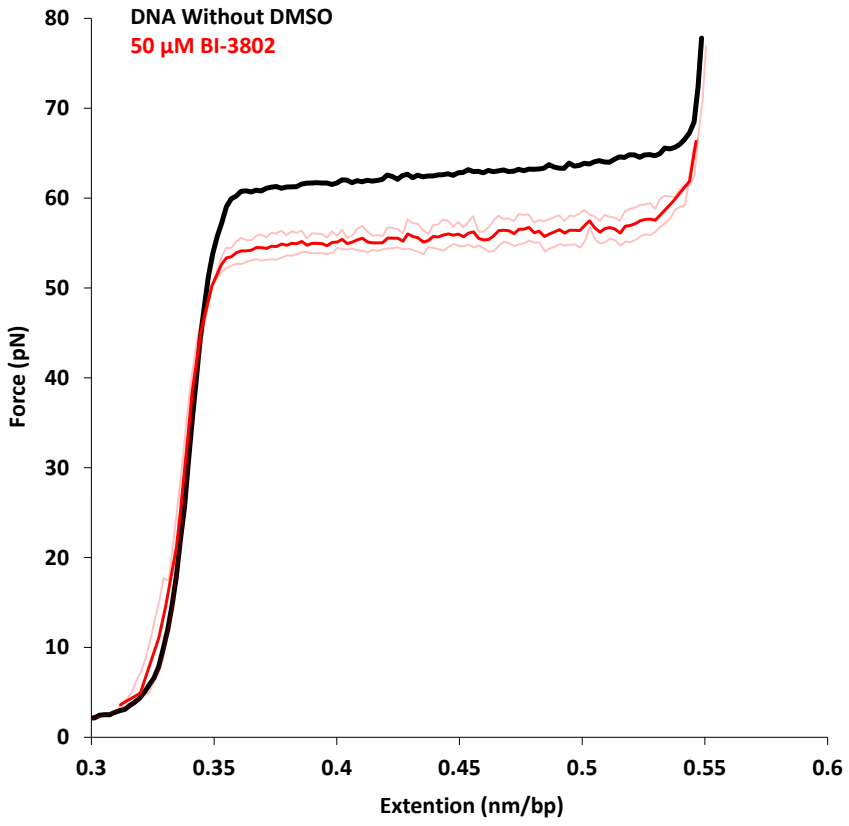

Figure 38: Force versus Extension graph displaying the stretching of a single DNA molecule without BI-3802 added (black curve) compared with the stretching of 2 DNA molecules in the presence of 50 µM of BI-3802 (light red curves) that are averaged into one curve (dark red curve).

The averaged DNA stretching curves from the three concentrations of BI-3802 were all put into one graph to compare with the DNA stretched in the presence of the buffer alone in Figure 39. The graph shows, with increased BI-3802 concentrations, the force required to melt the dsDNA is decreased. This means that BI-3802 is facilitating the separation of the DNA base pairs during the melting transition, showing that BI-3802 destabilizes the structure of dsDNA.

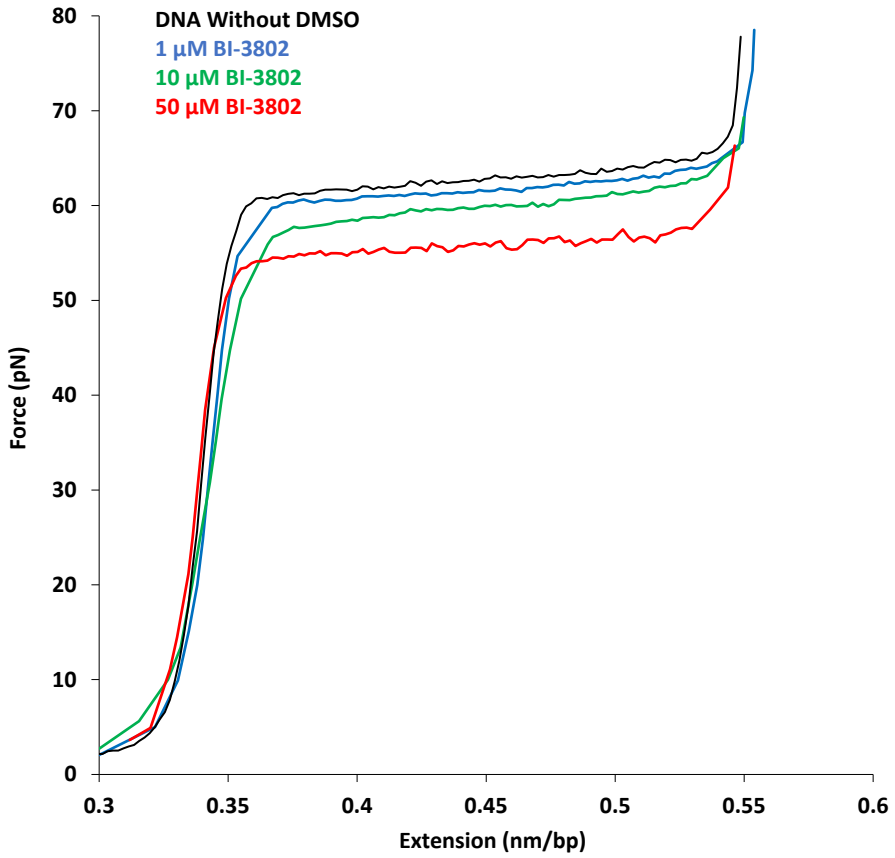

Figure 39: Force versus Extension graph displaying the averaged curves from stretching DNA in the presence of 1 µM (blue curve), 10 µM (green curve), and 50 µM (red curve) concentrations of BI-3802 along with the curve obtained from stretching DNA in buffer alone (black curve).

Discussion

BI-3802 is a recently developed small molecule drug that is believed to target transcription repressor BCL6 and lead to the regression of the most common form of lymphatic cancer, B-cell lymphoma. Based on the molecular structure of BI-3802 it looks like an intercalator, a special type of molecule which has a flat planar section that can stack between DNA base pairs. The goal of this research project was to explore the interaction of BI-3802 with DNA, which to our knowledge has never been done. We used optical tweezers to isolate single DNA molecules to study the interactions of BI-3802.

BI-3802 is dissolved in the solvent Dimethyl Sulfoxide (DMSO). Since DMSO based drugs had not yet been studied in our lab, some preliminary tests using DMSO were done before conducting the BI-3802 experiments. By obtaining the optical tweezers trap stiffness in the presence of increasing volume ratios of DMSO: buffer we found that the trap stiffness is only affected by DMSO after the threshold ratio of 5:2000, DMSO: buffer. This is most likely due to DMSO changing the refractive index of the medium. We then moved on to our next preliminary test, DNA molecules were stretched in the presence of increasing volumes of DMSO until an effect was observed. After the ratio 5:2000, DMSO: buffer the DNA stretching curve began to be affected. The force required to melt the dsDNA was decreased, the DMSO was facilitating the DNA melting. This shows that the DMSO was destabilizing the structure of dsDNA after the mentioned ratio. The preliminary tests told us that if we stay under the threshold ratio of 5:2000, DMSO: buffer our experiments would not be affected by DMSO.

We then moved on to explore the interactions of BI-3802 with DNA, it was found BI-3802 binds to DNA in mM range. We were able to collect data on DNA stretched in the presence of three different BI-3802 concentrations (1 µM, 10 µM, and 50 µM) before exceeding the previously mentioned DMSO threshold. With increased BI-3802 concentrations, the force required to melt the dsDNA was decreased. This means BI-3802 is facilitating the separation of the DNA base pairs during the melting transition, showing that BI-3802 destabilizes the structure of dsDNA.

This is the first time anyone has observed the interaction of BI-3802 with DNA. Many anti-cancer drugs that are used during chemotherapy can also bind to DNA in non-cancerous cells and cause side effects. Therefore, understanding the DNA binding is not only important to see the drugs binding mechanism, but also to identify the side effects of the drug. In the case of BI-3802, our experiments show that it begins to interact with DNA at micro molar (µM) concentrations. However, this drug is administered in the nM range to target BCL6, therefore the patient should not see any side effects due to the interaction with DNA.

In general, intercalators increase the force required to melt the DNA and also show significant lengthening of the dsDNA. However, BI-3802 did not show any of these effects and in contrast it lowered the melting force. Even though BI-3802 did not behave like an intercalator as we expected before starting the project, it still binds to DNA at µM concentrations, and the good news is, at the current nM dosage, there should not be any side effects through binding to DNA. These binding characteristics can potentially be used to help further develop new drugs that are similar to BI-3802.

References

1 Urry, L. A. *et al. Campbell biology*. Eleventh edition. edn, (Pearson Education, Inc., 2017).

2 Johannsen, W. The Genotype Conception of Heredity. *The American Naturalist* **45**, 129-159 (1911). https://doi.org:10.1086/279202

3 Paramanathan, T. *Drug-DNA interactions at single molecule level: A view with optical tweezers*, Northeastern University, (2010).

4 Avery, O. T., Macleod, C. M. & McCarty, M. Studies on the Chemical Nature of the Substance Inducing Transformation of Pneumococcal Types: Induction of Transformation by A Deoxyribonucleic Acid Fraction Isolated from Pneumococcus Type III. *J Exp Med* **79**, 137-158 (1944). https://doi.org:10.1084/jem.79.2.137

5 Franklin, R. E. & Gosling, R. G. Evidence for 2-chain helix in crystalline structure of sodium deoxyribonucleate. *Nature* **172**, 156-157 (1953). https://doi.org:10.1038/172156a0

6 Watson, J. D. & Crick, F. H. Molecular structure of nucleic acids; a structure for deoxyribose nucleic acid. *Nature* **171**, 737-738 (1953). https://doi.org:10.1038/171737a0

7 Wilkins, M. H., Stokes, A. R. & Wilson, H. R. Molecular structure of deoxypentose nucleic acids. *Nature* **171**, 738-740 (1953). https://doi.org:10.1038/171738a0

8 Pray, L. A. Discovery of DNA Structure and Function: Watson and Crick. *Nature Education* **1**, 100 (2008).

9 Levene, P. The structure of yeast nucleic acid. *Studies from the Rockefeller Institute for Medical Research* **30** (1919).

10 Chargaff, E., Lipshitz, R., Green, C. & Hodes, M. E. The composition of the deoxyribonucleic acid of salmon sperm. *J Biol Chem* **192**, 223-230 (1951).

11 Kerres, N. *et al.* Chemically Induced Degradation of the Oncogenic Transcription Factor BCL6. *Cell Rep* **20**, 2860-2875 (2017). https://doi.org:10.1016/j.celrep.2017.08.081

12 Liu, D. *et al.* Circulating apoptotic bodies maintain mesenchymal stem cell homeostasis and ameliorate osteopenia via transferring multiple cellular factors. *Cell Research* **28**, 918-933 (2018). https://doi.org:10.1038/s41422-018-0070-2

13 *The Lymphatic System and Cancer*, <https://www.cancerresearchuk.org/what-is-cancer/body-systems-and-cancer/the-lymphatic-system-and-cancer> (

14 Dotan, E., Aggarwal, C. & Smith, M. R. Impact of Rituximab (Rituxan) on the Treatment of B-Cell Non-Hodgkin's Lymphoma. *P t* **35**, 148-157 (2010).

15 Cardenas, M. G. *et al.* The Expanding Role of the BCL6 Oncoprotein as a Cancer Therapeutic Target. *Clin Cancer Res* **23**, 885-893 (2017). https://doi.org:10.1158/1078-0432.CCR-16-2071

16 Nutt, S. L., Hodgkin, P. D., Tarlinton, D. M. & Corcoran, L. M. The generation of antibody-secreting plasma cells. *Nature Reviews Immunology* **15**, 160-171 (2015). https://doi.org:10.1038/nri3795

17 Dougherty, T. J. & Pucci, M. J. *Antibiotic discovery and development*. (Springer, 2012).

18 Chu, S. Arthur Ashkin (1922–2020): Physicist who won Nobel for optical tweezers that trap atoms and proteins. *Nature* **588** (2020).

19 *Steven Chu - Facts*, <https://www.nobelprize.org/prizes/physics/1997/chu/facts/> (2022).

20 Ashkin, A., Dziedzic, J. M. & Yamane, T. Optical trapping and manipulation of single cells using infrared laser beams. *Nature* **330**, 769-771 (1987). https://doi.org:10.1038/330769a0

21 Wang, M. D., Yin, H., Landick, R., Gelles, J. & Block, S. M. Stretching DNA with optical tweezers. *Biophys J* **72**, 1335-1346 (1997). https://doi.org:10.1016/S0006-3495(97)78780-0

22 Bustamante, C. J., Chemla, Y. R., Liu, S. & Wang, M. D. Optical tweezers in single-molecule biophysics. *Nat Rev Methods Primers* **1** (2021). https://doi.org:10.1038/s43586-021-00021-6

23 Townes-Anderson, E., St Jules, R. S., Sherry, D. M., Lichtenberger, J. & Hassanain, M. Micromanipulation of retinal neurons by optical tweezers. *Mol Vis* **4**, 12 (1998).

24 Walker, L. M. *et al.* Mechanical manipulation of bone and cartilage cells with 'optical tweezers'. *FEBS Lett* **459**, 39-42 (1999). https://doi.org:10.1016/s0014-5793(99)01169-2

25 Vorobjev, I. A., Liang, H., Wright, W. H. & Berns, M. W. Optical trapping for chromosome manipulation: a wavelength dependence of induced chromosome bridges. *Biophys J* **64**, 533-538 (1993). https://doi.org:10.1016/s0006-3495(93)81398-5

26 Bar-Ziv, R., Moses, E. & Nelson, P. Dynamic excitations in membranes induced by optical tweezers. *Biophys J* **75**, 294-320 (1998). https://doi.org:10.1016/s0006-3495(98)77515-0

27 Zhu, R., Avsievich, T., Popov, A. & Meglinski, I. Optical Tweezers in Studies of Red Blood Cells. *Cells* **9** (2020). https://doi.org:10.3390/cells9030545

28 Ells, Z. *Quantifying Anticancer Drug Doxorubicin Binding to DNA Using Optical Tweezers*, Bridgewater State University, (2020).

29 Jabak, A. A. *The Effect of Chirality on DNA Threading: Exploring Binuclear Ruthenium Intercalators Using Optical Tweezers*, Bridgewater State University, (2020).

30 Watts, J. *Using Optical Tweezersto Probe DNA Polymerase Kappa's Binding Mechanism to DNA*, Bridgewater State University, (2022).

31 Adam, A. J. *et al.* Left versus right: Exploring the effects of chiral threading intercalators using optical tweezers. *Biophysical Journal* **121**, 3745-3752 (2022). https://doi.org:https://doi.org/10.1016/j.bpj.2022.04.025

32 Ashkin, A. Acceleration and Trapping Particle by Radiation Pressure. *Physical Review Letters* **24**, 156-159 (1970).

33 Williams, M. C., Wenner, J. R., Rouzina, I. & Bloomfield, V. A. Effect of pH on the overstretching transition of double-stranded DNA: evidence of force-induced DNA melting. *Biophys J* **80**, 874-881 (2001). https://doi.org:10.1016/S0006-3495(01)76066-3

34 Chaurasiya, K. R., Paramanathan, T., McCauley, M. J. & Williams, M. C. Biophysical characterization of DNA binding from single molecule force measurements. *Phys Life Rev* **7**, 299-341 (2010). https://doi.org:10.1016/j.plrev.2010.06.001

35 McCauley, M. J., Chaurasiya, K. R., Paramanathan, T., Rouzina, I. & Williams, M. C. DNA stretching as a probe for nucleic acid interactions: Reply to Comments on "Biophysical characterization of DNA binding from single molecule force measurements" by Kathy R. Chaurasiya, Thayaparan Paramanathan, Micah J. McCauley, Mark C. Williams. *Phys Life Rev* **7**, 358-361 (2010). https://doi.org:10.1016/j.plrev.2010.07.008

36 Bustamante, C., Bryant, Z. & Smith, S. B. Ten years of tension: single-molecule DNA mechanics. *Nature* **421**, 423-427 (2003). https://doi.org:10.1038/nature01405

37 Fu, H., Chen, H., Marko, J. F. & Yan, J. Two distinct overstretched DNA states. *Nucleic Acids Res* **38**, 5594-5600 (2010). https://doi.org:10.1093/nar/gkq309

38 Bryant, Z. *et al.* Structural transitions and elasticity from torque measurements on DNA. *Nature* **424**, 338-341 (2003). https://doi.org:10.1038/nature01810

39 Leger, J. *et al.* Structural transitions of a twisted and stretched DNA molecule. *Physical review letters* **83**, 1066 (1999).

40 Williams, M. C., Wenner, J. R., Rouzina, I. & Bloomfield, V. A. Entropy and heat capacity of DNA melting from temperature dependence of single molecule stretching. *Biophys J* **80**, 1932-1939 (2001). https://doi.org:10.1016/S0006-3495(01)76163-2

41 Williams, M. C. *et al.* Mechanism for nucleic acid chaperone activity of HIV-1 nucleocapsid protein revealed by single molecule stretching. *Proc Natl Acad Sci U S A* **98**, 6121-6126 (2001). https://doi.org:10.1073/pnas.101033198

42 van Mameren, J. *et al.* Unraveling the structure of DNA during overstretching by using multicolor, single-molecule fluorescence imaging. *Proc Natl Acad Sci U S A* **106**, 18231-18236 (2009). https://doi.org:10.1073/pnas.0904322106

43 Vladescu, I. D., McCauley, M. J., Rouzina, I. & Williams, M. C. Mapping the phase diagram of single DNA molecule force-induced melting in the presence of ethidium. *Phys Rev Lett* **95**, 158102 (2005). https://doi.org:10.1103/PhysRevLett.95.158102

44 Casjens, S. R. & Hendrix, R. W. Bacteriophage lambda: Early pioneer and still relevant. *Virology* **479-480**, 310-330 (2015). https://doi.org:10.1016/j.virol.2015.02.010

45 Daudelin, B. *Advanced Dual Beam Optical Tweezers for Undergraduate Biophysics Research*, Bridgewater State University, (2016).

46 LeBel, R. G. & Goring, D. A. I. Density, Viscosity, Refractive Index, and Hygroscopicity of Mixtures of Water and Dimethyl Sulfoxide. *Journal of Chemical & Engineering Data* **7**, 100-101 (1962). https://doi.org:10.1021/je60012a032

47 Tunçer, S. *et al.* Low dose dimethyl sulfoxide driven gross molecular changes have the potential to interfere with various cellular processes. *Sci Rep* **8**, 14828 (2018). https://doi.org:10.1038/s41598-018-33234-z

48 Bryden, N. *Quantifying the DNA Binding Properties of the Binuclear Ruthenium Complex ΛΛ-P*, Bridgewater State University, (2016).